To the Graduate Council:

I am submitting herewith a dissertation written by James Robert Merriman, entitled "Analysis of a Multicomponent Gas Absorption System with Carrier Gas Coabsorption." I recommend that it be accepted in partial fulfillment of the requirements for the degree of Doctor of Philosophy, with a major in Chemical Engineering.

J. J. Perona, Major Professor

We have read this dissertation
and recommend its acceptance:

Accepted for the Council:

Vice Chancellor
Graduate Studies and Research

ANALYSIS OF A MULTICOMPONENT GAS ABSORPTION SYSTEM WITH CARRIER GAS COABSORPTION

A Dissertation

Presented for the

Doctor of Philosophy

Degree

The University of Tennessee

James Robert Merriman

March 1975

ACKNOWLEDGMENTS

The author is indebted to several people who provided considerable help during the course of this project. In particular, the author's co-workers at the Oak Ridge Gaseous Diffusion Plant made invaluable contributions. Mr. D. L. Burkett coordinated the construction, installation, and operation of the pilot plant equipment; Mr. M. J. Stephenson supervised the experimental activities; Mr. J. H. Pashley was responsible for overall management of the work; and Dr. D. I. Dunthorn provided frequent and important technical guidance. Mr. Stephenson and Dr. Dunthorn also reviewed this dissertation as it progressed and made very helpful suggestions.

The author is also grateful to his advisor, Dr. J. J. Perona, for suggesting the overall framework for the dissertation and for recommending the basic calculational approaches. Dr. Perona's patience during a long project is also appreciated.

1214651

ABSTRACT

Conventional integrated versions of the packed gas absorber design equations do not account for significant coabsorption of the carrier gas along with the dilute transferring species. These equations, as a result, also neglect the relationship between dilute component transfer and carrier gas coabsorption. In the absorption of Kr and Xe from various carrier gases, using CCl_2F_2 as the process solvent, carrier coabsorption is substantial. Consequently, a design package was developed to deal with multicomponent gas absorption in systems characterized by carrier gas coabsorption. Developed within the general film theory framework, the basic feature of this design approach is a view of dilute component mass-transfer as a conventional diffusive transfer superimposed on a net flux caused by carrier absorption. Other supporting elements of the design package include predictive techniques for various fluid properties, estimating procedures for carrier gas equilibrium constants, and correlations for carrier gas and dilute gas mass-transfer coefficients. When applied to systems using CCl_2F_2 as the solvent; He, N_2, air, or Ar as the carrier gas; and Kr or Xe as the dilute gas; the design approach gave good results, even when extended to conditions well beyond those of its development.

TABLE OF CONTENTS

CHAPTER		PAGE
I.	INTRODUCTION	1
	Background	1
	Problem Statement	4
II.	FUNDAMENTAL SOLVENT AND SOLUTE PROPERTIES	8
	Introduction	8
	Solvent Properties	8
	Solute Properties	9
	Binary Gas Mixture Properties	9
	Liquid-Phase Diffusion Coefficients	16
	Solubility of Gases in CCl_2F_2	17
	Reported solubility data	17
	Alternatives	24
	Estimating procedures	26
	Ranges of predicted K_i^* values for gases in CCl_2F_2	41
	Choice of estimated constants	41
III.	EXPERIMENTAL APPARATUS AND TEST RESULTS	55
	Absorption System Design	55
	Pilot plant process description	55
	Absorber column design	58
	Experimental Data	58
IV.	ANALYTICAL PROCEDURES	61
	Introduction	61
	Governing Equations	62

CHAPTER PAGE

Summary of Calculational Procedures 64

Some Additional Definitions 65

V. CARRIER GAS MASS-TRANSFER DATA 69

Introduction 69

Mass-Transfer Coefficients 71

Sensitivity Analysis 76

VI. DILUTE GAS MASS-TRANSFER DATA 78

Introduction 78

Experimental Data Reduction 81

Diffusive Transfer Data 82

Total Dilute Gas Transfer 85

Summary 91

VII. MIXED CARRIER GAS MASS-TRANSFER DATA 93

Introduction 93

Analysis of Air Tests 94

Extension of Results 95

VIII. CONCLUSION 104

LIST OF REFERENCES 108

APPENDIX 111

VITA 119

LIST OF TABLES

TABLE		PAGE
I.	Selected Physical Properties of CCl_2F_2	10
II.	Selected Physical Properties of Solutes	11
III.	Viscosity Parameters for Carrier Gases	14
IV.	Typical Binary Gas Mixture Parameters	15
V.	Example Liquid-Phase Diffusion Coefficients and Schmidt Numbers for CCl_2F_2 Systems at -25°F	18
VI.	Summary of Equilibrium Constants Derived from Reported Data on the Solubility of Various Gases in CCl_2F_2	20
VII.	Comparison of ORGDP Liquid-Phase Mole Fractions with BNL-UT Saturation Values	22
VIII.	Solubility Parameters for Gaseous Solutes	30
IX.	Internal Energy of Vaporization of Solutes at Their Normal Boiling Points	33
X.	Solubility Parameters for Gases Dissolved in $C_2Cl_3F_3$ at 25°C	34
XI.	Predicted Equilibrium Constants for Gases in CCl_2F_2 Based on Their Solubilities in $C_2Cl_3F_3$	37
XII.	Solubility Parameters for Selected Solvents at 25°C	40
XIII.	Solubilities of Gases in $(C_4F_9)_3N$	42
XIV.	Selected Binary Equilibrium Constants for Gases in CCl_2F_2	52
XV.	Summary of Experimental Data	60
XVI.	Liquid-Phase Mass-Transfer Coefficients	72
XVII.	Summary of K_La Correlating Groups	74

TABLE		PAGE
XVIII.	Summary of Sensitivity Analysis	77
XIX.	Dilute Component Gas-Phase Mass-Transfer Coefficients . .	83
XX.	Summary of Possible Relationships Between $K_g a$ and Various Parameters	84
XXI.	Summary of Air Test Results	96
XXII.	Comparison of Absorption Experiments Using CCl_2F_2 Solvents	98
XXIII.	Extension of Results to Stephenson's Experiments	100
XXIV.	Comparison of Kr-Air-CCl_2F_2 and CO_2-Air-Water Systems . .	105

LIST OF FIGURES

FIGURE		PAGE
1.	Solubility Data for Gases in $C_2Cl_3F_3$	36
2.	Divergence of Solubility Values for $(C_4F_9)_3N$ from Regular Solution Line	43
3.	Entropy of Solution of Gases in $(C_4F_9)_3N$	44
4.	Predicted Equilibrium Constants for He in CCl_2F_2	45
5.	Predicted Equilibrium Constants for N_2 in CCl_2F_2	46
6.	Predicted Equilibrium Constants for O_2 in CCl_2F_2	47
7.	Predicted Equilibrium Constants for Ar in CCl_2F_2	48
8.	Predicted Equilibrium Constants for Kr in CCl_2F_2	49
9.	Predicted Equilibrium Constants for Xe in CCl_2F_2	50
10.	Selected Equilibrium Constants for Various Gases in CCl_2F_2	54
11.	Krypton-Xenon Absorption Process Pilot Plant Schematic Flow Diagram	56
12.	Profile Data for Test Series 3	66
13.	Profile Data for Test Series 4	67
14.	Comparison of Measured and Correlated Diffusive Gas-Phase Mass-Transfer Coefficients Using Equation (43)	86
15.	Comparison of Measured and Correlated Diffusive Gas-Phase Mass-Transfer Coefficients Using Equation (44)	87
16.	Comparison of Actual and Predicted Total Gas-Phase Mass-Transfer Coefficients	90
17.	Concentration and Gas Flow Profiles for Test 15	97
18.	Kr Concentration Profiles	103

CHAPTER I

INTRODUCTION

I. BACKGROUND

In a typical nuclear power reactor, up to 300 grams of Kr and 4700 grams of Xe, per metric ton of fuel, are formed in the fuel during its irradiation (Merriman, 1966). A small portion of this material migrates from the fuel during reactor operation, and the remainder is released when the fuel is sheared and dissolved during reprocessing. Because of this, removal of Kr and Xe from off-gas streams which their radioactive isotopes contaminate is becoming of increasing concern in the nuclear industry, as efforts are mounted to reduce all radioactive discharges to levels which are as low as practicable.

A number of processes have been proposed for controlling the discharge of noble gases from nuclear facilities. Among these are off-gas holdup processes, which employ delay tanks or charcoal adsorption beds to introduce sufficient residence time prior to atmospheric release to permit decay of the short half-life (less than 5.3 days) Kr and Xe isotopes; cryogenic distillation processes, which remove the Kr and Xe from the carrier gas; and selective absorption processes, which also separate and reclaim the noble gases from the carrier in a concentrated form suitable for long-term storage or further processing. Physical separation processes, using either distillation or absorption, are required whenever ^{85}Kr control is necessary, due to the relatively

long half-life (10.7 years) of this isotope. For this reason, the separation processes have more general applicability than holdup processes.

The selective absorption technique for Kr-Xe recovery is being studied in an ongoing engineering development program at the Oak Ridge Gaseous Diffusion Plant (ORGDP). This work was initiated in 1967 and is sponsored by the United States Energy Research and Development Administration, under Contract W-7405-eng-26 with the Nuclear Division of Union Carbide Corporation. In the absorption process, a carrier gas stream, containing varying but small quantities of Kr and Xe, is introduced to the bottom of a packed gas absorber column, operated at conditions under which essentially complete dissolution of the noble gas in the downflowing solvent occurs. This leaves the absorber off-gas free of Kr and Xe, allowing this stream to be vented to the atmosphere. Simultaneously, however, a significant amount of carrier gas also dissolves, and the next step in the process involves passing the loaded solvent to an intermediate stripper column. The intermediate stripper is designed and operated to achieve virtually complete desorption of the coabsorbed carrier gas and thereby increase the proportion of Kr and Xe in the residual dissolved gas. The off-gas from this unit, which contains some Kr and Xe in addition to the stripped carrier gas, is recycled to the absorber. The liquid which exits from the intermediate stripper contains dissolved gas which is enriched in Kr and Xe, and this stream is subsequently routed to a final stripper. In the final stripper, Kr and Xe are evolved and collected as a concentrated gas product, with the lean solvent returned to the top of the absorber column.

The goal of the ORGDP program is demonstration of the general feasibility of the selective absorption process for effective Kr and Xe removal. This is being accomplished through pilot plant experiments which simulate, as closely as possible, the actual processing conditions typical of potential commercial applications of the process to specific types of nuclear reactors and fuel reprocessing plants. Accordingly, the ORGDP work has focused primarily on the relationships between overall Kr-Xe removal efficiency and system operating variables, such as temperature, pressure, and gas and liquid flow rates. Since the range of potential applications is wide, the experimental conditions have also covered relatively large regions. For example, a number of different carrier gases have been utilized; Kr and Xe concentrations in the feed have varied over several orders of magnitude; other trace impurities have been introduced to the system; absorption pressures and temperatures have ranged from about 11 to 35 atm and -75 to +25°F, respectively; feed gas flow rates have been between 1 and 22 scfm; solvent flow rates have been from 1 to 2 gpm; and two different fluorocarbon solvents have been employed. The results of the program to date have been very favorable, indicating that the selective absorption process has considerable potential for efficient Kr-Xe removal under a variety of specific application conditions (Merriman, et al., 1972). The more versatile solvent has been found to be CCl_2F_2, at typical absorption conditions of 25 atm and -25°F. In addition, it has been observed that this general type of process, using other fluorocarbon solvents, might be of considerable value in various nonnuclear gas separation problems requiring high recovery efficiencies (Merriman, et al., 1973, 1974).

II. PROBLEM STATEMENT

From a chemical engineering standpoint, the most distinguishing feature of the selective absorption process for Kr and Xe, using fluorocarbon solvents, is the substantial and unusual amount of carrier gas which coabsorbs with the desired components in the absorber column. As an illustration, in the experiments described in this dissertation up to 75 percent of the carrier was dissolved in the absorber along with the noble gas. This represents a considerable departure from the more usual class of gas absorption problems. The most common packed absorber column design approaches for simple binary gas systems, for example, are addressed to a feed gas containing a soluble component to be recovered from an insoluble carrier gas. Even the more complex multicomponent system design equations, such as those based on solutions of the Stefan-Maxwell equations, customarily assume that the carrier for the multiple soluble components is itself insoluble (Toor and Sebulsky, 1961). These approaches have been successful in describing a large number of absorption systems, and the usual impact of considering increased numbers of components is increased calculational complexity, rather than any change in the broad point of view.

The practical difference between having a soluble carrier gas, as opposed to an insoluble one, can be illustrated by considering a two-component gas stream containing the carrier plus the desired dilute species. When the carrier is insoluble, the mass-transfer rate equation and the material balance equation can ordinarily be readily combined and integrated to yield relatively simple design equations relating column

height to flow rates, the equilibrium constant for the dilute component, and terminal mole fractions of the soluble component in the two phases. The more soluble the carrier is, on the other hand, the more the gas and liquid flow rates vary throughout the column. The lack of a constant carrier gas flow precludes the customary integration of the design equations, and use of the standard integrated forms to describe the behavior of the dilute component requires that some assumption be made regarding the "best" flow rate values to use. For example, in the ORGDP work, where Kr-Xe removal was the primary concern, averaged inlet and outlet flow rates were assumed in calculating the numbers of transfer units for the noble gases using conventional integrated design equations (Merriman, et al., 1972). While this type of treatment eventually yielded acceptable empirical relationships between overall Kr-Xe removal efficiency and system variables, it greatly compromises the real picture of what is occurring with respect to the noble gas absorption. Furthermore, the approaches which use standard integrated models or their graphical equivalents are of no validity in describing the behavior of the coabsorbed carrier, and they totally neglect the important relationship between carrier coabsorption and dilute component absorption.

With the above points in mind, it was decided to undertake the development of a comprehensive absorber design package applicable to the general problem of multicomponent gas absorption in systems containing soluble carrier gases. The general guideline established for this work was that it be derived, insofar as possible, from an accepted chemical engineering model of the fundamental absorption process. Accordingly,

the two-film theory was chosen as the basic framework. The specific objectives of the project included:

1. Selecting procedures for obtaining the necessary basic physical property data,
2. Developing a design approach which satisfactorily accounts for coabsorption of one or more carrier gases without restrictive physical or mathematical assumptions,
3. Combining the above with a design approach which not only characterizes the absorption of the desired dilute components, but also relates this absorption back to the carrier coabsorption, and
4. Testing the total design package against data taken outside the ranges of parameters used in the development of the various procedures.

The dissertation is based on a series of absorption experiments in which CCl_2F_2 was used as the process solvent. Coabsorbing carrier gases included He, N_2, Ar, and air, and the desired dilute components were Kr and Xe. The absorber temperature was in the neighborhood of -25°F, with the pressure varied between about 21 and 29 atm.

A final point which merits elaboration is that prior to development of the mass-transfer design package for this absorption system, it was necessary to pursue at some length estimation of equilibrium constants for the various gases of interest. This was due to the limited amount of reported equilibrium data available, which appeared to conflict substantially with direct ORGDP results and with data on solubilities of gases in other fluorocarbons, and which also did not appear to be

thermodynamically consistent. In a more fundamental sense, the previously reported results on the solubilities of gases in CCl_2F_2 also did not appear to address the recognized effects of additional components on binary equilibrium constants. Since it was desired in this project to formally account for these third-component effects, an important initial objective was selection of a procedure which could be used for estimating consistent equilibrium data for various gases, either pure or in mixtures, in CCl_2F_2. As described in the next chapter, the form of the equilibrium constant used in this work is the component gas-phase fugacity divided by the component liquid-phase mole fraction, and the estimating model selected accounts for temperature, pressure, and third-component effects on binary solubility constants.

CHAPTER II

FUNDAMENTAL SOLVENT AND SOLUTE PROPERTIES

I. INTRODUCTION

In the analysis and correlation of experimental data, having good values of fundamental fluid properties is, of course, of crucial importance. The situation in this project was somewhat complicated by the fact that the test conditions, typically -25°F and 25 atm, were removed from the regions where most physical property data are best known. Also, virtually no data exist at any conditions on liquid diffusion coefficients for the systems of interest here. Furthermore, and perhaps most important, it was found necessary to select a procedure for estimating consistent equilibrum data, as mentioned in the previous chapter.

For these reasons, and because it is hoped that this dissertation can be used as a design guide for further studies of similar absorption problems, a considerable effort was made to identify good basic data and good estimating methods for cases where good data were not available. This chapter is a summary of the data and predictive techniques considered to be most applicable to the problem of absorption of gases in CCl_2F_2.

II. SOLVENT PROPERTIES

The solvent used in this work was dichlorodifluoromethane, CCl_2F_2, commonly referred to as "Refrigerant-12." Tabulations of basic

properties of CCl_2F_2 are extensive; the data used in this analysis were taken from two Du Pont references (McHarness, et al., 1955; Du Pont, 1956). Key physical properties are summarized in Table I.

Liquid density and viscosity values were obtained from equations developed to fit the Du Pont data, as follows:

$$\rho_L = 34.84 + 0.02696\ (693.3\text{-}T) + 0.834921\ (693.3\text{-}T)^{1/2} + 6.02683\ (693.3\text{-}T)^{1/3} - 6.55549 \times 10^{-6}\ (693.3\text{-}T)^2 \quad (1)$$

where ρ_L [=] pounds/ft^3, and

T [=] °R ;

and $$\mu_L = .018679 \exp \frac{1289.8}{T} , \quad (2)$$

where μ_L [=] cp, and

T [=] °R.

III. SOLUTE PROPERTIES

Several gases were used in the experiments, namely He, N_2, O_2, Ar, Kr, and Xe. Typically, a dilute gas, Kr or Xe, was mixed with a bulk carrier gas, He, N_2, air, or Ar, to prepare feed gas mixtures for the absorption tests. Selected properties of these gases are listed in Table II.

IV. BINARY GAS MIXTURE PROPERTIES

The most important gas mixture properties for this problem are those required to calculate the gas-phase Schmidt number, Sc_g. Diffusion coefficients were estimated using the following series of equations (Bretsznajder, 1971):

TABLE I

Selected Physical Properties of CCl_2F_2

Property	Value
Molecular Weight	120.93
Normal Boiling Point, °F	-21.62
V_b, ft^3/lb mole	1.302
T_c, °F	233.6
P_c, atm	40.6
V_c, ft^3/lb mole	3.471
σ at +40°F, dynes/cm	11.8
μ_L at -40°F, cp	0.398
Enthalpy of Vaporization at -40°F, Btu/lb mole	8817

Source: Du Pont, 1956.

TABLE II

Selected Physical Properties of Solutes

Property	Value for Indicated Gas						
	He	Air	N_2	O_2	Ar	Kr	Xe
Molecular Weight	4	28.97	28.02	32.00	39.944	83.80	131.3
T_c, °K	5.26	132	126.2	154.4	151	209.4	289.8
P_c, atm	2.26	36.4	33.5	49.7	48.0	54.3	58.0
V_c, cc/g-mole	57.8	86.6	90.1	74.4	75.2	92.2	118.8
Lennard-Jones Parameters[a]:							
σ, Å	2.576	3.617	3.681	3.433	3.418	3.61	4.055
ε/k, °K	10.2	97.0	91.5	113	124	190	229

[a]From viscosity data.

Source: Bird, et al., 1960.

$$D_{AB} = \frac{BT^{3/2}}{P\sigma_{AB}^2 \Omega_{AB}} \left(\frac{M_A + M_B}{M_A M_B} \right)^{1/2} , \quad (3)$$

$$B = 0.00214 - 0.000492 \left(\frac{M_A + M_B}{M_A M_B} \right)^{1/2} , \quad (4)$$

$$\Omega_{AB} \doteq 1.075 \left(\frac{kT}{\epsilon_{AB}} \right)^{-0.1615} + 2 \left(\frac{10\ kT}{\epsilon_{AB}} \right)^{F} , \quad (5)$$

$$F = -0.3214 \ln \left(\frac{10\ kT}{\epsilon_{AB}} \right) , \quad (6)$$

$$\sigma_{AB} = \frac{1}{2} (\sigma_A + \sigma_B), \text{ and} \quad (7)$$

$$\epsilon_{AB} = (\epsilon_A \epsilon_B)^{1/2} ; \quad (8)$$

where D_{AB} [=] cm^2/sec,

T [=] °K,

M_A, M_B = molecular weights of pure gases A and B, and

$\sigma_A, \sigma_B, \epsilon_A, \epsilon_B$ = Lennard-Jones parameters for pure gases A and B, with the conventional units of Å and °K, respectively.

Viscosities of pure gases were estimated using known values at 273°K and the following relationship (Bretsznajder, 1971):

$$\mu_T = \mu_0 \frac{(273 + C)}{(T + C)} \left[\frac{T}{273}\right]^{3/2}, \qquad (9)$$

where T [=] °K, and

C = Sutherland constant.

Values of μ_0 and C for the bulk gases used in the experiments are given in Table III. It can be seen that neither composition nor pressure dependencies have been accounted for in equation (9). Furthermore, the Sutherland constants themselves are functions of temperature over broad temperature ranges. However, the Sutherland constants given in Table III are adequate for the calculations required in this project, since the experimental temperatures were substantially closer to 0°C, where the constants were obtained, than to temperatures where significant changes in the constants occur. Additionally, the composition dependencies are insignificant since in all of the experiments the dilute component, Kr or Xe, was present at mole fractions of 10^{-6} or less in the bulk gas. Finally, examination of N_2 viscosity data indicates that the pressure dependence can be practically ignored at the pressures (25 atm) used in the tests with little error (less than 3 percent).

Using the above relationships, binary gas mixture parameters can be calculated. Some typical numbers at 25 atm and -25°F are presented in Table IV.

In the cases just described, it can be noted that air has been treated as a single pure gas. Alternative considerations are mentioned in a later chapter.

TABLE III

Viscosity Parameters for Carrier Gases

Gas	Vicosity at 0°C, poises x 10^6	Sutherland Constant
He	188.5	80
Air	170.8	112
N_2	165.2	104
O_2	191.1	125
Ar	211.4	142

Source: Bretsznajder, 1971.

TABLE IV

Typical Binary Gas Mixture Parameters[a]

System	$\rho \times 10^3$, g/cm^3	$\mu \times 10^6$, g/cm-sec	$D_{AB} \times 10^3$, cm^2/sec	PD_{AB}, atm-cm^2/sec	Sc_g
Kr-He	5.05	172	18.3	0.457	1.86
Kr-N_2	35.4	150	4.52	0.113	0.937
Kr-Air	36.6	155	4.50	0.113	0.940
Xe-Air	36.6	155	3.68	0.092	1.15
Kr-Ar	50.4	190	4.07	0.102	0.927

[a]Calculated at 25 atm and -25°F.

V. LIQUID-PHASE DIFFUSION COEFFICIENTS

There is no completely rigorous way to treat diffusion in liquid systems. Also, experimental data for diffusion of gases in liquids are not plentiful, and are nonexistent for many systems of interest. As a result, empirical correlations are required to estimate values of the liquid-phase diffusion coefficient, D_L, for dilute solutions of the diffusing solute. The correlation used here is the one developed by Wilke and Chang (Wilke and Chang, 1955):

$$D_L = 7.2 \times 10^{-8} \frac{T(XM_2)^{1/2}}{\mu V_b^{0.6}}, \qquad (10)$$

where T [=] ^{o}K,

M_2 = molecular weight of solvent,

μ = viscosity of solvent, cp,

X = association parameter for the solvent = 1 for CCl_2F_2, and

V_b = molal volume of solute at normal boiling point, cc/g mole.

In applying equation (10), the choice of V_b values is open to some question, due to scatter in the reported literature values and uncertainties related to the treatment of He. For purposes of consistency, at least, in these calculations, V_b values were calculated from the V_c values given in Table II, page 11, using the relationship $V_b/V_c \doteq 0.38$ (Hildebrand, 1969).

It is apparent that calculated diffusion coefficients for gases dissolved in CCl_2F_2 will be higher than analogous coefficients for aqueous solutions, due to the higher molecular weight and lower viscosity of CCl_2F_2 compared with water. The absolute accuracy of equation (10) for gas-CCl_2F_2 systems is unknown. However, the method is conventionally used in chemical engineering analysis and is consistently applied here.

In Table V, example values of D_L and Sc_L are given for the bulk gas-CCl_2F_2 liquid solutions of interest in this work.

VI. SOLUBILITY OF GASES IN CCl_2F_2

Reported Solubility Data

A few measurements of the solubilities of various gases in CCl_2F_2 have been made at two laboratories, Brookhaven National Laboratory (BNL) and the University of Tokyo (UT) (Steinberg, 1959; Yamamoto and Takeda, 1970). The BNL data were obtained using various techniques, including flowing gas through a fixed volume of liquid until the inlet and outlet component flows became equal, and then integrating to obtain the quantity of gas absorbed. The UT measurements were made using an autoclave to equilibrate a fixed charge of gas and liquid at a high pressure, after which the liquid was depressurized and component outgas flows were measured. The BNL data for N_2, Ar, and O_2 were taken using "pure" gases containing only traces of noble gas; corresponding data for Kr and Xe were collected using dilute concentrations of radioactive isotopes of these gases in N_2. The UT experiments were all made using a three-component gas mixture of N_2, O_2, and Kr, from which binary

TABLE V

Example Liquid-Phase Diffusion Coefficients and Schmidt Numbers for CCl_2F_2 Systems at -25°F

System	$D_L \times 10^5$, cm^2/sec	Sc_L
He-CCl_2F_2	8.46	28.7
Air-CCl_2F_2	6.66	36.5
N_2-CCl_2F_2	6.50	37.4
O_2-CCl_2F_2	7.28	33.4
Ar-CCl_2F_2	7.23	33.6

parameters were obtained. The combined measurements at BNL and UT covered temperature and pressure ranges bracketing those used in this dissertation.

Both the BNL and UT data were reported in terms of Ostwald coefficients, or volume of absorbed gas corrected to standard temperature and pressure per volume of solvent at the temperature of experiment per atmosphere. The BNL data were also reported in terms of Henry's law constants. Corrections for gas-phase departures from ideality at the relatively high experimental pressures were made by the UT investigators, but appear to have been ignored in the BNL work. Consequently, before analysis, the BNL data were reconstructed by inverting the reported BNL data reduction procedure and then corrected back using the appropriate fugacity coefficients. The resulting binary equilibrium contants are summarized in Table VI. In Table VI, and for convenience throughout this dissertation, the equilibrium constant is defined by the following equation:

$$K_i^* = \frac{f_i^G}{x_i} , \tag{11}$$

where K_i^* = equilibrium constant, atm,

f_i^G = gas-phase fugacity, atm, and

x_i = liquid-phase mole fraction .

There is some noticeable scatter in the BNL and UT data, even recognizing the temperature and pressure ranges involved. Also, much of the data, particularly the UT mixture data, does not represent true measurement of binary equilibrium constants. Furthermore, in these

TABLE VI

Summary of Equilibrium Constants Derived from Reported Data on the Solubility of Various Gases in CCl_2F_2

Gaseous Component	Measurement Conditions T, °K	P_T, atm	Gas-Phase Concentration of Component	K_1^*, atm	Laboratory
N_2	197.6	5.41	100%	486	BNL
	240.2	6.7	~80%	(730)	UT
	240.2	54	~80%	(480)	UT
	240.2	80	~80%	(440)	UT
	243.2	5.52	100%	664	BNL
	276.2	5.87	100%	583	BNL
O_2	197.2	3.92	100%	217	BNL
	237.2	4.22	100%	354	BNL
	240.2	6.7	~20%	(400)	UT
	240.2	54	~20%	(300)	UT
	240.2	80	~20%	(250)	UT
	274.2	5.85	100%	393	BNL
Ar	200.2	3.69	100%	175	BNL
	227.2	4.75	100%	254	BNL
	273.2	5.96	100%	312	BNL
Kr	190.2	5.51	74 ppm	22.9	BNL
	193.2	11.4	74 ppm	25.2	BNL
	197.6	7.12	74 ppm	27.9	BNL
	240.2	6.7	~2000 ppm	(69)	UT
	240.2	54	~2000 ppm	(71)	UT
	240.2	70	~2000 ppm	(75)	UT
	240.2	80	~2000 ppm	(77)	UT
	244.2	5.62	74 ppm	56.9	BNL
	273.2	3.47	74 ppm	114	BNL
Xe	196.2	9.07	5050 ppm	5.7	BNL
	273.2	6.41	5050 ppm	37	BNL

Sources: Steinberg, 1959; Yamamoto and Takeda, 1970.

cases, no attempts appeared to be made by the investigators to compensate for any effects of additional components on their reported binary constants. These factors prevented a thorough analysis here of the binary systems to retrieve liquid-phase activity coefficients, for example. Serious problems with these numbers also arise because of discrepancies between the data for N_2, O_2, and Ar and ORGDP measurements, discrepancies between these data and solubility data for the same gases in other fluorocarbons, and an apparent lack of thermodynamic consistency. Each of these points is discussed briefly in the following sections.

Discrepancies with ORGDP data. The most obvious problem with the BNL and UT data for N_2, O_2, and Ar is the apparent conflict between the data and direct measurements made in the ORGDP program. The measured liquid-phase mole fractions of carrier gases dissolved in the solvent leaving the absorption column in the ORGDP work have always been found to be higher than the limiting equilibrium, or saturation, mole factions indicated by the BNL-UT data. This fact is illustrated in Table VII, where measured mole fractions and indicated saturation values are compared for a few typical experiments. The ORGDP values represent a very large number of data points collected over several years in different equipment and verified through independent techniques with material balance checks, whereas the BNL-UT data for N_2, O_2, and Ar represent only 15 points. The suggestion is that the latter data either are not correct or are not sufficiently detailed to permit uncoupling third-component liquid-phase effects which might be significant in this system. In either case, there still remains the practical problem of not

TABLE VII

Comparison of ORGDP Liquid-Phase Mole Fractions with BNL-UT Saturation Values

Test Series	Gas	Liquid-Phase Mole Fractions	
		ORGDP Measurements	BNL-UT Saturation Limits
M-1	N_2	0.046	0.035
M-7	N_2	0.060	0.042
M-12	Ar	0.10	0.088
S-1	Air	0.083	0.055
S-7	Air	0.088	0.055
S-13	Air	0.059	0.033
S-19	Air	0.053	0.037
S-25	Air	0.073	0.041
S-31	Air	0.069	0.056

Sources: This work, for runs prefixed with M, and Stephenson, et al., 1970, for runs prefixed with S.

having a way to obtain consistent equilibrium constants based on the reported data.

Discrepancies with other data. A second point lending some support to the inadequacy of the BNL-UT data is the difference between this data and data on the solubility of gases in other fluorocarbon solvents. While this is certainly only a qualitative comparison, the BNL-UT data for the solubility of N_2 in CCl_2F_2 appear about 50 percent lower than Hildebrand's data for the solubility of N_2 in $C_2Cl_3F_3$ (Hildebrand and Lamoreaux, 1974), whereas the simple theory suggests that the reverse should be the case. The data for Ar solubility in the two liquids show a similar, but smaller variation. Comparisons with perfluoro solvent data reflect even larger differences (e.g., Powell, 1972).

Thermodynamic consistency. A final consideration important in the critical examination of the reported solubility data for N_2, O_2, and Ar is its apparent lack of thermodynamic consistency. A test procedure developed by Adler was used to evaluate the BNL-UT N_2 data (Adler, et al., 1960). This procedure was specifically devised for checking binary liquid-vapor equilibrium data when one component is above its critical temperature. To summarize very briefly, a rigorous form of the Duhem equation, including corrections for nonideality in the vapor phase, was employed; this introduced a third term, or a "correction" term, to the more common two-term version of the Gibbs-Duhem equation. Numerically, the test involves comparison of the sum of two areas obtained through graphical integration with the area corresponding to the correction term. To be consistent, the sum of

the first two areas, $A_1 + A_2$, should equal the third area, A_3. Application of this test requires either isothermal or isobaric binary data. Since this was not directly available for CCl_2F_2 solutions, the BNL-UT data for N_2 were empirically related to temperature and pressure using least squares techniques. The resulting fit was used to produce isothermal points at -25°F, and these points were then employed in the consistency test. This test was only applied to the N_2 data, because this is the carrier gas of most interest and because the primary goal at this juncture was to double-check the earlier conclusions regarding the inadequacy of the reported carrier gas solubility data. The final results of the test gave an $A_1 + A_2$ value of -5.92 versus an A_3 value of -4.41. This difference indicates rather poor thermodynamic consistency, even without quantitative guidance regarding what degree of agreement is required for "good" versus "bad" data.

Based on all the above considerations, it was concluded that the reported solubility data for N_2, O_2, and Ar in CCl_2F_2 were not directly applicable to this dissertation project.

Alternatives

Having identified a need for improved equilibrium constants for N_2, O_2, and Ar in CCl_2F_2, it was necessary to consider possible choices for obtaining such numbers. The scope, timetable, and funding of the ORGDP project precluded any substantial effort at direct measurement. Consequently, only two options remained. One alternative was simply to assume arbitrary equilibrium constants which did not predict liquid-phase saturation mole fractions below the observed absorber column

exit data. The second alternative was to estimate equilibrium constants according to some accepted technique. The latter course appeared more defensible and offered the promise of obtaining more consistent numbers, so it was chosen.

The next problem was identification of the specific technique to be used for estimating the equilibrium constants. There are many different models which have been employed to predict K-values for various vapor-liquid systems, but none has been found to be universally applicable. The methods selected for the dissertation were all based on the regular solution theory framework developed by Hildebrand.[1] This framework has been used with various modifications to correlate and predict a fair amount of equilibrium data, including some hydrocarbon mixture data by Chao and Seader and various gas solubility data (Prausnitz, 1969). A further important factor in the selection of this general model, however, was the fact that Hildebrand has also done most of the reported work on the measurement and correlation of gas solubility data in fluorocarbons. It is not claimed that the regular solution approach represents the best technique for predicting K-values for all systems. Rather, it was judged that the model constituted an attractive way to estimate values for the CCl_2F_2 systems of interest. To be as conservative as possible, however, even within the regular solution theory framework two different approaches were generally taken, with two variations of each approach considered. This resulted in four sets of estimated equilibrium constants which were viewed as enveloping

---

[1] Technically, both Scatchard and Hildebrand independently proposed the basic elements of the regular solution theory.

the values which would be useful in the project. As discussed in the following sections, the first approach combines the regular solution equation for the activity coefficient with the theorem of corresponding states to establish "regular" values of the solubilities of interest. The second approach uses Hildebrand's correlations to predict solubility limits.

Estimating Procedures

Regular solution theory. Only an outline of the regular solution theory is presented here, since details are contained in a recent text by Prausnitz (Prausnitz, 1969). Fundamentally, a regular solution, as defined by Hildebrand, is one in which components mix with no excess entropy in the absence of volume changes. Working from van Laar's equations, a new parameter is introduced to free these equations from the van der Waals or any other equation of state. This new parameter, δ, is defined by;

$$\delta^2 = \frac{\Delta E^V}{V_L} , \tag{12}$$

where ΔE^V = internal energy of vaporization, and

V_L = liquid molal volume.

Implicit in the regular solution theory is the assumption that the dispersion force-related parameters can be simply combined as suggested by London's formula, viz:

$$\delta_{12}^2 = \delta_1 \delta_2 . \tag{13}$$

Using these concepts and basic thermodynamics relationships, the following important equation for the solute activity coefficient can be derived:

$$RT \ln\gamma_2 = V_2\Phi_1^2[\delta_1 - \delta_2]^2 , \tag{14}$$

where γ_2 = solute activity coefficient, and

Φ_1 = solvent volume fraction,

with subscripts 1 and 2 referring to solvent and solute, respectively.

Next, the isothermal dissolution in a liquid of a gaseous component at fugacity f^G is postulated as a two-step process. In the first step, the gas "condenses" to the volume which it has as a dissolved solute. In the second step, the solute and solvent are mixed. Writing the free energies for these steps gives:

$$\Delta g = \Delta g_I + \Delta g_{II} = 0 \text{ at equilibrium,} \tag{15}$$

$$\Delta g_I = RT \ln \frac{f_2^L}{f_2^G} , \text{ and} \tag{16}$$

$$\Delta g_{II} = RT \ln \gamma_2 x_2 ; \tag{17}$$

where f_2^L = fugacity of the hypothetical liquid solute (pure) following "condensation."

Combining equations (15), (16), and (17), with the regular solution relationship, equation (14), gives:

$$K_2^* = \frac{f_2^G}{x_2} = f_2^L \exp\left[\frac{V_2^L (\delta_1 - \delta_2)^2 \phi_1^2}{RT}\right] , \tag{18}$$

where the superscript "L" has been added in V_2^L to emphasize that this is a hypothetical liquid molar volume of the dissolved solute gas.

Values for f_2^L, the fugacity of the hypothetical liquid, can be obtained from corresponding-states plots or, alternatively, from the following empirical equation:

$$\frac{f_2^L}{P_C} = 26252.0 \exp\left[\frac{-7.047}{T_r} - 4.8264\ T_r + 1.568\ T_r^2 - 0.2107\ T_r^3\right] . \tag{19}$$

Equation (19) was obtained by least-squares fitting the f^L versus P_C curves presented by various authors (e.g., Yen and McKetta, 1962).

At pressures substantially higher than one atmosphere, the f_2^L values obtained from equation (19) need to be multiplied by the Poynting correction:

$$\exp\left[\frac{V_2^L (P - 1)}{RT}\right] , \tag{20}$$

before use in equation (18). Finally, for mixtures of solvents, or for high solute concentrations, the form of equation (18) is:

$$K_2^* = f_2^L \exp\left[\frac{V_2^L (\bar{\delta} - \delta_2)^2}{RT}\right] , \tag{21}$$

where

$$\bar{\delta} \equiv \sum_i \phi_i \delta_i , \tag{22}$$

and the summation is over all components, including the solutes.

Use of equations (18) through (22) was made to modify the binary constants for various pressures and various concentrations of other dissolved solutes. In practice, these corrections were not large, numerically.

Practically, equation (18) is a correlating equation based on a theoretical model, rather than a strict a priori estimating equation. This is because the solute parameters, V_2 and δ_2, cannot be directly measured. On the other hand, solvent parameters, V_1 and δ_1, are readily available so considerable use has been made of the model to fit experimental solubility data and thereby obtain correlated values for the solute parameters. Having values for V_2 and δ_2 based on extensive solubility data for gases in various solvents, and knowing values for V_1 and δ_1 for a solvent of interest for which no solubility data exist, equation (18) usually provides a satisfactory estimate of solubilities for gas-liquid pairs whose other physical properties (such as polarity) do not greatly violate the assumptions inherent in the regular solution theory.

Values of the solubility parameters for several gases have been reported by Prausnitz and Shair (Prausnitz and Shair, 1961). Additional values, reportedly based on the correlation of more experimental data, including some data for fluorocarbon systems, were obtained by Yen and McKetta (Yen and McKetta, 1962). Values from both efforts are given in Table VIII for the gases of interest in this work. In using the regular solution theory to estimate CCl_2F_2 constants, both sets of values were used, together with the following values for CCl_2F_2:

TABLE VIII

Solubility Parameters for Gaseous Solutes[a]

Gas	Obtained by Prausnitz and Shair V_2, cc/mole	Obtained by Prausnitz and Shair δ_2, $(cal/cc)^{1/2}$	Obtained by Yen and McKetta V_2, cc/mole	Obtained by Yen and McKetta δ_2, $(cal/cc)^{1/2}$
N_2	32.4	2.58	40.0	3.20
O_2	33.0	4.0	49.6	4.70
Ar	57.1	5.33	55.0	5.00
Kr	65	6.4	52.0	5.90
Xe			45.8	6.30

[a]Based on solubilities of gases in n-C_7F_{16}, $(C_4F_9)_3N$, C_7F_{14}, C_8F_{16}, i-C_8H_{18}, n-C_6H_{14}, n-C_7H_{16}, n-C_8H_{18}, C_7H_{14}, c-C_6H_{12}, CCl_4, C_6H_6, and CS_2.

Sources: Prausnitz and Shair, 1961; Yen and McKetta, 1962.

$$V_1 = 92.4 \text{ cc/mole, and}$$

$$\delta_1 = 6.05 \text{ (cal/cc)}^{1/2} .$$

Hildebrand's correlations. In recent years, Hildebrand and co-workers have provided graphic correlations of solubility data based on the fact that, for gases which obey Henry's law, the entropy of solution and the change of solubility with temperature are related by:

$$\bar{S}_2 - S_2^g = R\left(\frac{\partial \ln x_2}{\partial \ln T}\right)_p . \tag{23}$$

Plots of $-R\ln x_2$ at 25°C and 1 atm versus $\bar{S}_2 - S_2^g$ have been found to give a straight line for various gases dissolved in a particular solvent. Lines for different solvents vary, but the slopes, s, for most regular solvents have been found to be related to the solubility parameter as follows:

$$s-1 = 0.90 - 0.004\delta_1^2 . \tag{24}$$

While the slopes of the lines for different solvents vary, the lines for all those solvents for which accurate data are available tend to converge to $\bar{S}_2 - S_2^g = -21$ cal/mole-°K at $-R\ln x_2 = 0$. At this point, where $x_2 = 1$, with $x_1 = 0$, Hildebrand has noted that the value, -21 cal/mole-°K, represents the entropy associated with condensing a gas whose boiling point at one atmosphere is 25°C (Hildebrand and Lamoreaux, 1974).

Using this intercept as a base for the partial molal entropy, Hildebrand has defined a quantity, ΔS_2^E, as the excess partial molal entropy (above -21 cal/mole-°K), viz:

$$\Delta\bar{S}_2^E = (\bar{S}_2 - S_2^g) + 21 \quad . \tag{25}$$

Further considering the entropy as related not only to concentration changes but also to changes in attraction forces, another parameter, the configuration entropy, $\Delta\bar{S}^C$, has been defined by:

$$\Delta\bar{S}^C = R\ln x_2 + \Delta\bar{S}^E \quad . \tag{26}$$

Finally, in Hildebrand's correlations, use is made of a basic solute property, namely, the internal energy of vaporization at the boiling point, ΔE^V. Values of ΔE^V for the gases of interest are listed in Table IX. For the condensation of a gas whose boiling point at one atmosphere is 25°C, with an entropy of condensation of -21 cal/mole-°K, the internal energy of vaporization would be 5.67 kcal/mole.

In general, for a particular solute, values of $T\Delta\bar{S}^C$ have been found to show surprisingly small variation from solvent to solvent. Further, when $T\Delta\bar{S}^C$ values are plotted versus values of the solute quantity, $5.67 - \Delta E^V$, most data lie on a straight line of slope 1.81.

Considering the above framework as describing regular solution behavior, two variations were considered in estimating further equilibrium constants for CCl_2F_2 solubilities. In the first case, the slight departure from this pattern of $C_2Cl_3F_3$, the ethane analog of CCl_2F_2, was used as a basis for estimating constants for CCl_2F_2. In the second case, the dramatic departure of perfluoro solvents from the regular pattern was used as the estimating basis.

Fairly extensive data, summarized in Table X, are available on the solubilities of various gases in $C_2Cl_3F_3$ (Linford and Hildebrand, 1970;

TABLE IX

Internal Energy of Vaporization of Solutes at Their Normal Boiling Points

Solute	ΔE^V, kcal/mole
He	0.018
N_2	1.18
O_2	1.45
Ar	1.385
Kr	2.00
Xe	2.69

Source: Hildebrand and Lamoreaux, 1974.

TABLE X

Solubility Parameters for Gases Dissolved in $C_2Cl_3F_3$ at 25°C

Gas	ΔE^v, kcal/mole	$5.67-\Delta E^v$, kcal/mole	$T\Delta\bar{S}^c$, kcal/mole	$-RT\ln x_2$, kcal/mole
H_2	0.175	5.495	3.03	4.33
He	0.018	5.652	3.31	4.74
Ne	0.37	5.30	3.16	4.50
N_2	1.18	4.49	2.60	3.71
Ar	1.385	4.285	2.42	3.46
CH_4	1.73	3.940	2.19	3.13
Xe	2.69	2.98	1.60	2.28
C_2H_6	3.15	2.52	1.47	2.10

Source: Hildebrand and Lamoreaux, 1974.

Hildebrand and Lamoreaux, 1974). Plotted in Figure 1, the data lie just below the customary line of slope 1.81 and more nearly on a line of slope 1.75. If it is assumed that CCl_2F_2 likewise does not follow the regular pattern but, instead, deviates slightly like its analog, another set of solubility estimates can be made for gases in CCl_2F_2. Since the only departures from regular behavior in this case are assumed to be slight ones, it is reasonable to assume further that $T\Delta\bar{S}^c$ values can be obtained from the line in Figure 1, and that the slope of the $-R\ln x_2$ versus $\bar{S}_2 - S_2^g$ line can be calculated using the CCl_2F_2 solubility parameter, δ_1, in equation (24). This provides a slope of 1.75 for this line also.

The steps used now to estimate equilibrium constants in CCl_2F_2 and their variation with temperature are illustrated in Table XI. First, the gases of interest in this dissertation are listed together with their ΔE^v values. Corresponding $T\Delta\bar{S}^c$ values (where T = 298°K) are obtained by dividing by 1.75, the slope of the line in Figure 1. In turn, the $T\Delta\bar{S}^c$ numbers are divided by 0.75 [which is s-1 for CCl_2F_2 from equation (24)] to yield $-RT\ln x_2$ values. From these numbers, finally, values of equilibrium constants at 298°K can be readily calculated.

Going back to equations (23), (25), and (26), it can be seen that R times the slope of the temperature dependency line is given by:

$$R\left(\frac{\partial \ln x_2}{\partial \ln T}\right)_p = -\frac{RT\ln x_2}{T} + \frac{T\Delta\bar{S}^c}{T} - 21 , \qquad (27)$$

where T = 298°K.

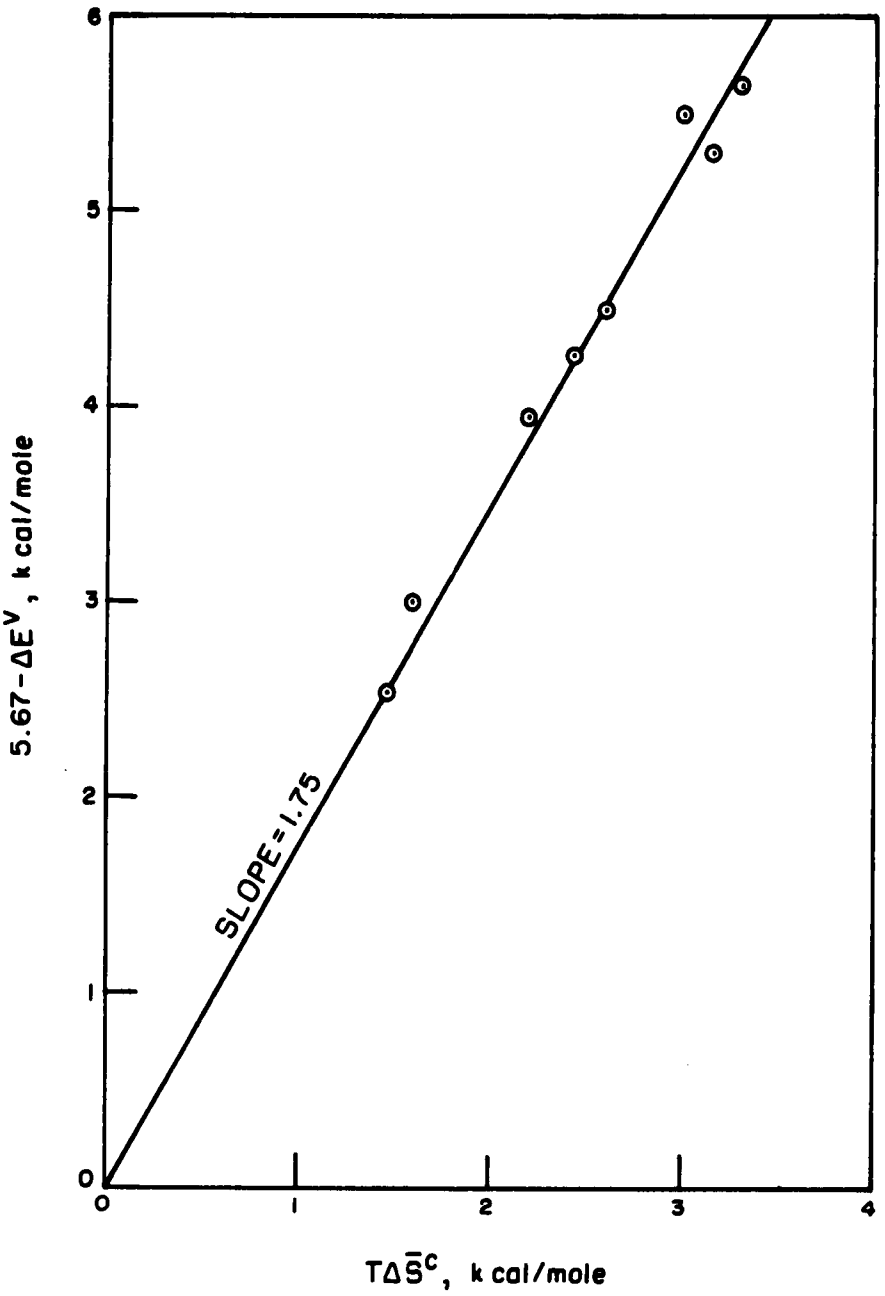


Figure 1. Solubility Data for Gases in $C_2Cl_3F_3$.

TABLE XI

Predicted Equilibrium Constants for Gases in CCl_2F_2 Based on Their Solubilities in $C_2Cl_3F_3$

Gas	ΔE^v, kcal/mole	$5.67-\Delta E^v$, kcal/mole	$T\Delta\bar{S}^c$ from Figure 1, kcal/mole[a]	$-RT\ln x_2$, kcal/mole[a]	Predicted K_i^* at 298°K, atm	Temperature Coefficient, β
He	0.018	5.652	3.230	4.307	1440	-2.16
N_2	1.18	4.49	2.566	3.421	323	0.458
O_2	1.45	4.22	2.411	3.215	228	1.07
Ar	1.385	4.285	2.449	3.265	248	0.919
Kr	2.00	3.67	2.097	2.796	112	2.31
Xe	2.69	2.98	1.703	2.271	46.3	3.86

[a]Temperature is 298°K.

A little further manipulation yields the following defining relationship for the temperature coefficient, β:

$$(K_i^*)_2 = (K_i^*)_1 \left(\frac{T_2}{T_1}\right)^{\beta} , \tag{28}$$

where $(K_i^*)_1$ = equilibrium constant at 298°K, atm,

$(K_i^*)_2$ = equilibrium constant at temperature T_2, atm,

T_1 = 298°K, and

T_2 = temperature of interest.

To sum up, in this case the only departures from regular solution behavior of the solubilities of gases in CCl_2F_2 are assumed to be analogous to the slight departures observed in $C_2Cl_3F_3$ systems. Note that this is not equivalent to saying that solubilities in CCl_2F_2 and $C_2Cl_3F_3$ are equal. Except for assuming that the slight shift from the regular pattern of the $T\Delta\bar{S}^c$ line is the same for the two solvents, the CCl_2F_2 parameters have been used in the regular manner.

In contrast, in numerous experiments, it has been found that solubilities of inert gases and alkanes in perfluoro solvents do not fit the regular solution pattern. In fact, Hildebrand has stated (Hildebrand and Lamoreaux, 1974) that:

> The lack of an adequate theory for these irregular interactions is the major block on the road to progress toward a general treatment of solutions. . . .

While CCl_2F_2 is not a perfluoro compound, its solubility parameter, δ_1, is nearly the same as δ_1 values for perfluoro solvents, although its molar volume, V_1, is considerably smaller. To illustrate, values of the

two solubility parameters, V_1 and δ_1, for various solvents are listed in Table XII.

The primary question is whether CCl_2F_2 behaves like perfluoro solvents or like more regular solvents. It is not possible to answer this question at the present time, because there is no complete understanding of what properties cause the anomalous behaviors of perfluoro compounds. If the perfluoro behavior is more or less associated with the rather large molal volumes, relative to hydrocarbon analogs, then the behavior of CCl_2F_2 would be expected to follow the more regular pattern described in the previous sections. If, however, the fluorocarbon behavior is more or less associated with the low vaporization energies, then the CCl_2F_2 behavior would be expected to follow the perfluoro compound pattern. It is because of this uncertainty that values of solubilities of gases in CCl_2F_2 cannot be estimated with the usual degree of confidence and that multiple approaches were employed in this dissertation. Because of the low δ_1 value of CCl_2F_2, perfluoro-like behavior has to be admitted as at least a possibility at this time. Since a goal of this section is to establish wide limits of predicted equilibrium constants, a second variation of Hildebrand's correlating models was pursued.

The most accurate solubility data for fluorocarbons appear to be for various gases in $(C_4F_9)_3N$ (Powell, 1972). Previous measurements using this and other perfluoro solvents had resulted in generally the same behavior for the solvents, even though the δ_1 values varied slightly from 5.9 to 6.1 $(cal/cc)^{1/2}$ (Hildebrand and Hirakoa, 1963). Consequently, the $(C_4F_9)_3N$ data offer a reasonable basis for estimating these boundary constants for CCl_2F_2 systems.

TABLE XII

Solubility Parameters for Selected Solvents at 25°C

Solvent	V_1, cc/mole	δ_1, $(cal/cc)^{1/2}$
C_6H_6	88.9	9.15
CCl_4	96.5	8.6
CCl_2F_2	92.4	6.05
$C_2Cl_3F_3$	120	7.24
C_7F_{16}	227	5.9
C_7F_{14}	196	6.0
C_8F_{16}	217	6.1
$(C_4F_9)_3N$		5.9

In Table XIII, the experimental data for various gases in $(C_4F_9)_3N$ are summarized, together with calculated (and interpolated) solubility parameters as previously defined. The experimental data are also plotted in Figures 2 and 3, to further illustrate the irregular behavior of fully fluorinated fluorocarbon solvents.

Ranges of Predicted K_i^* Values for Gases in CCl_2F_2

It should be apparent that a considerable effort has been made to provide as large an envelope as possible for estimated K_i^* values for gases in CCl_2F_2. In Figures 4 through 9, the different sets of predicted constants for He, N_2, O_2, Ar, Kr, and Xe are shown, as calculated using the regular solution equation, with both Prausnitz and Shair's and Yen and McKetta's parameters, as available, and using Hildebrand's correlating model, with both $C_2Cl_3F_3$-like and perfluoro-like irregularities. Also plotted are the reported experimental values and, for Kr and Xe, the saturation pressures for temperatures below the critical temperatures (International Critical Tables, 1928).

It can be seen that, if the terminal points are connected, relatively large regions are enscribed, which constitute areas in which defensible estimates could likely be chosen.

Choice of Estimated Constants

Having established broad regions for the estimated equilibrium constants, the task remains of proposing K_i^* values to use in analyzing the results from the absorption experiments. Fortunately, the temperature range of interest here, -80 to -10°F, is much more narrow than the range given in Figures 4 through 9, corresponding to lnT values in

TABLE XIII

Solubilities of Gases in $(C_4F_9)_3$ N

Gas	Solubility Data at 25°C: $10^4 x_2$	$\frac{R\,\partial \ln x_2}{\partial \ln T}$, cal/mole-°K	$5.67-\Delta E^v$, kcal/mole	$-RT\ln x_2$, kcal/mole	$T\Delta S^c$, kcal/mole	$\frac{T\Delta S^c}{-RT\ln x_2}$	K_i^* at 298°K, atm	Temperature Coefficient, β
He	11.67	4.13	5.652	3.999	3.490	0.87	857	-2.08
Ne	16.79	2.76	5.30	3.783	3.297	0.87		
Ar	61.05	-1.54	4.285	3.019	2.780	0.92	164	0.775
Kr	111.5	-3.30	3.67	2.662	2.613	0.98	89.7	1.66
Xe	215.2	-5.01	2.98	2.273	2.492	1.1	46.5	2.52
H_2	15.25	-3.28	5.495	3.830	3.405	0.89		
N_2	42.36	-0.35	4.49	3.235	2.919	0.90	236	0.176
CH_4	68.83	-1.88	3.94	2.948	2.750	0.93		
C_2H_6	227.4	-6.36	2.52	2.240	2.123	0.95		
O_2[a]		(-1.63)	4.22	(3.022)	(2.75)	(0.91)	(165)	0.820

[a]Values in parentheses for O_2 are interpolated.

Source: Powell, 1972.

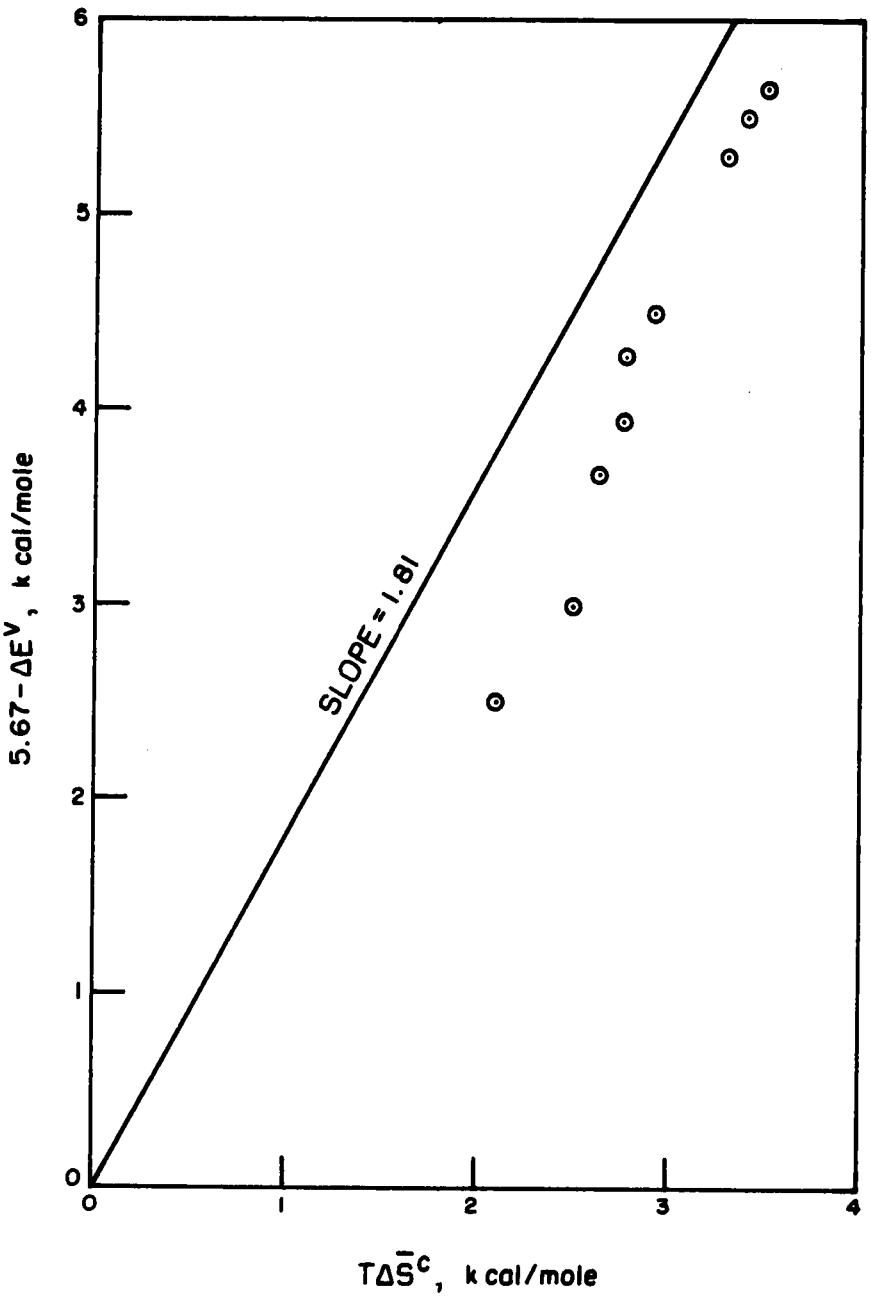


Figure 2. Divergence of Solubility Values for $(C_4F_9)_3N$ from Regular Solution Line.

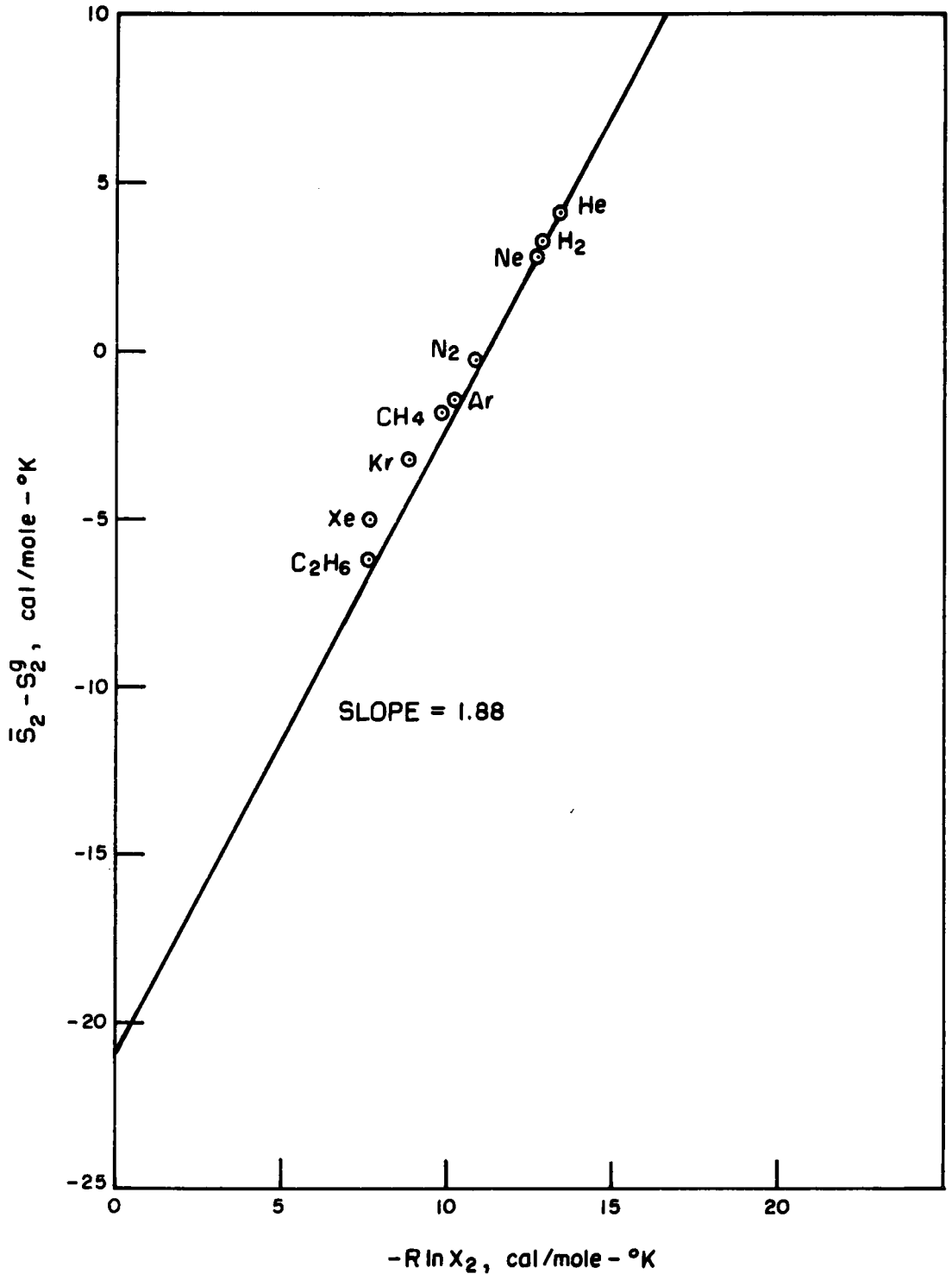


Figure 3. Entropy of Solution of Gases in $(C_4F_9)_3N$.

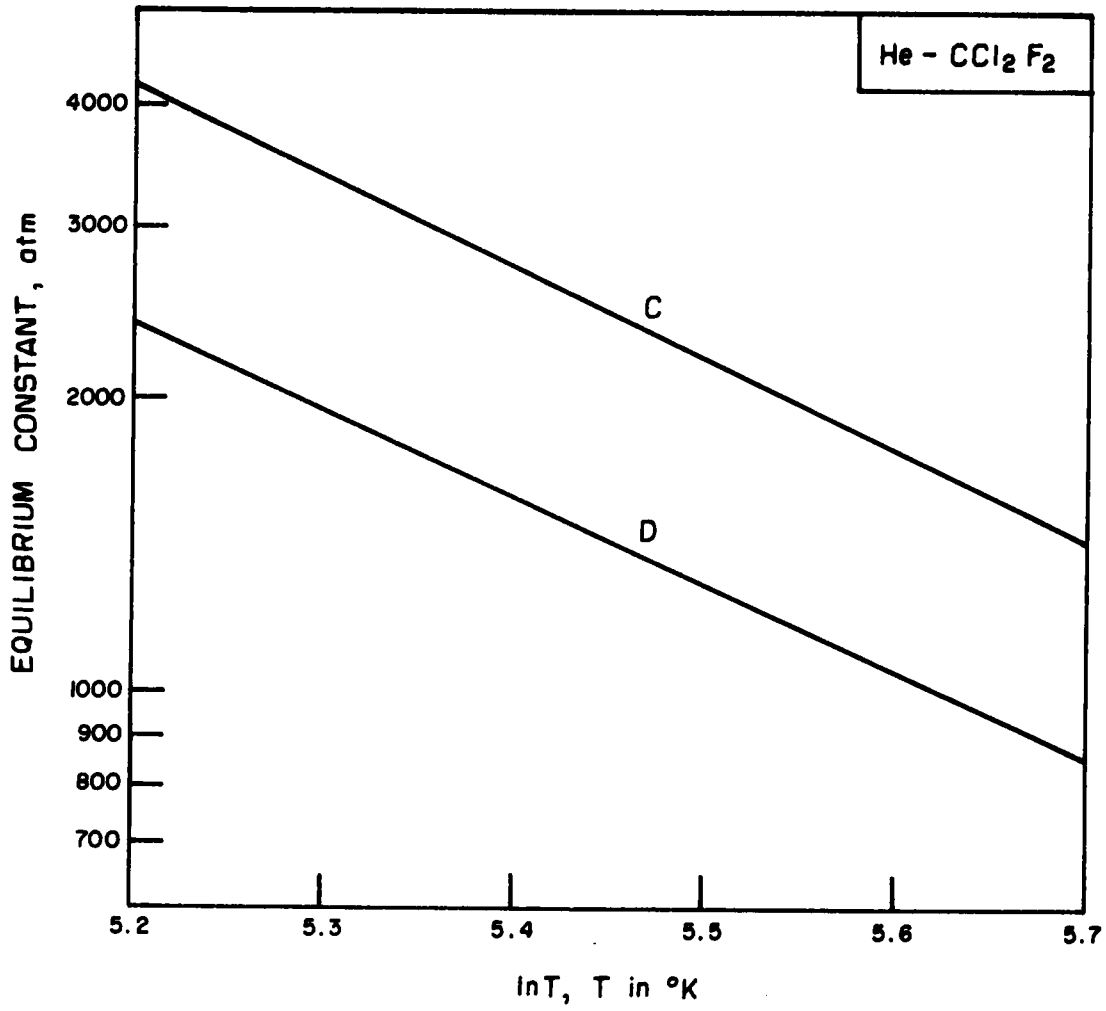


Figure 4. Predicted Equilibrium Constants for He in CCl_2F_2. Curve "C" is based on $C_2Cl_3F_3$ behavior. Curve "D" is based on perfluoro-solvent behavior.

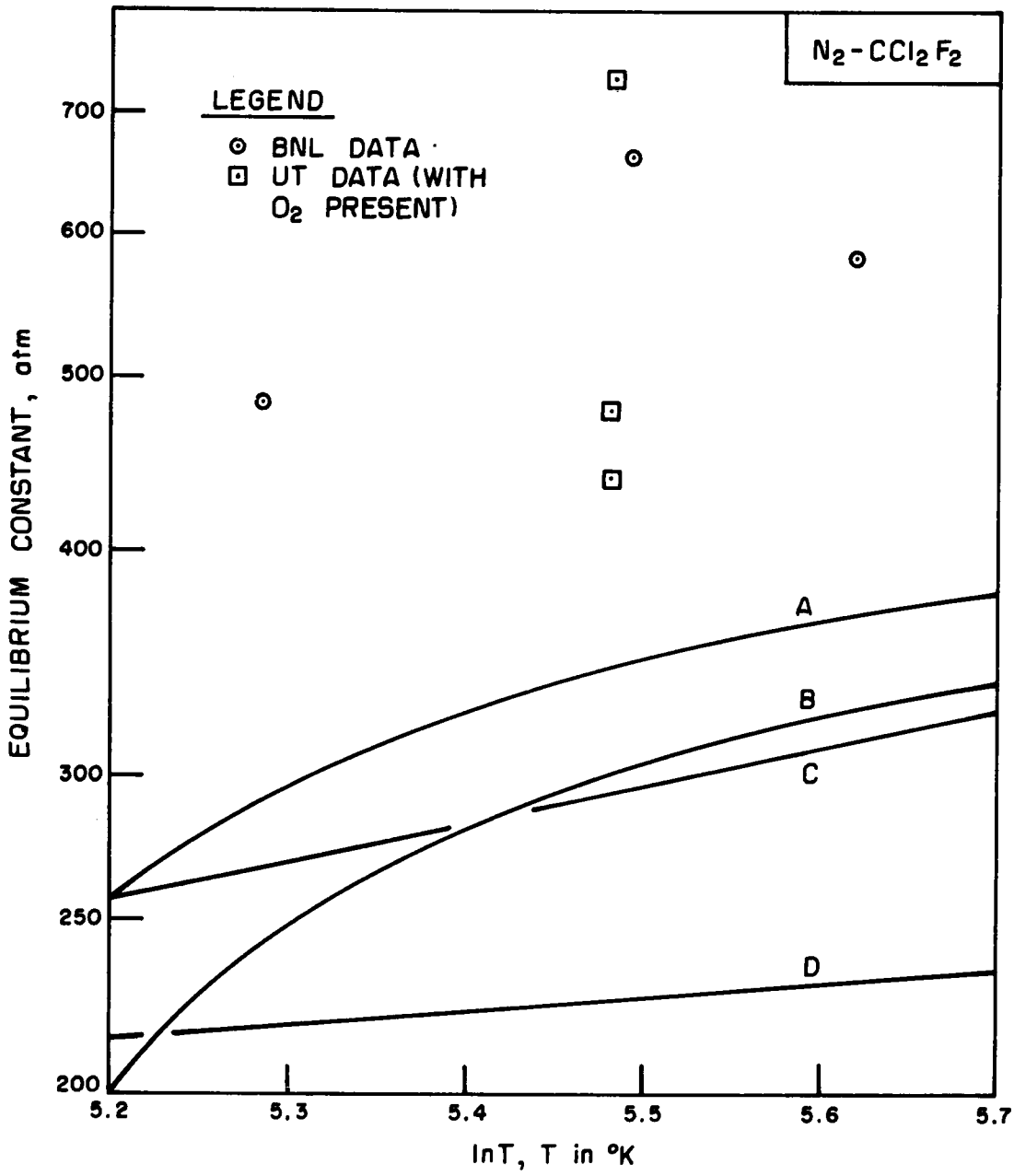


Figure 5. Predicted Equilibrium Constants for N_2 in CCl_2F_2. Curve "A" is based on the regular solution equations with Prausnitz and Shair's solubility parameters. Curve "B" is based on the same equations with Yen and McKetta's solubility parameters. Curve "C" is based on $C_2Cl_3F_3$ behavior. Curve "D" is based on perfluoro-solvent behavior.

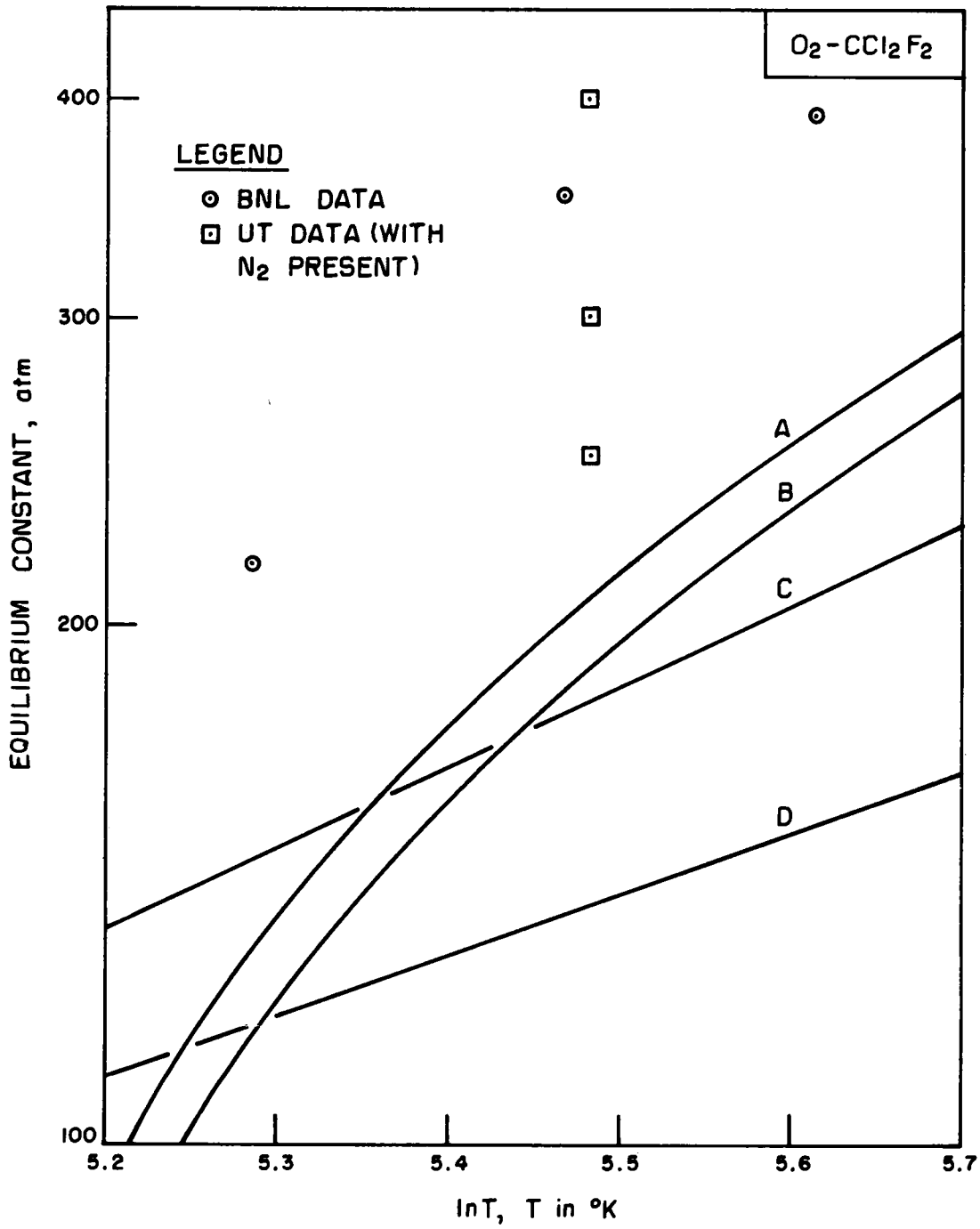


Figure 6. Predicted Equilibrium Constants for O_2 in CCl_2F_2. Curve "A" is based on the regular solution equations with Prausnitz and Shair's solubility parameters. Curve "B" is based on the same equations with Yen and McKetta's solubility parameters. Curve "C" is based on $C_2Cl_3F_3$ behavior. Curve "D" is based on perfluoro-solvent behavior.

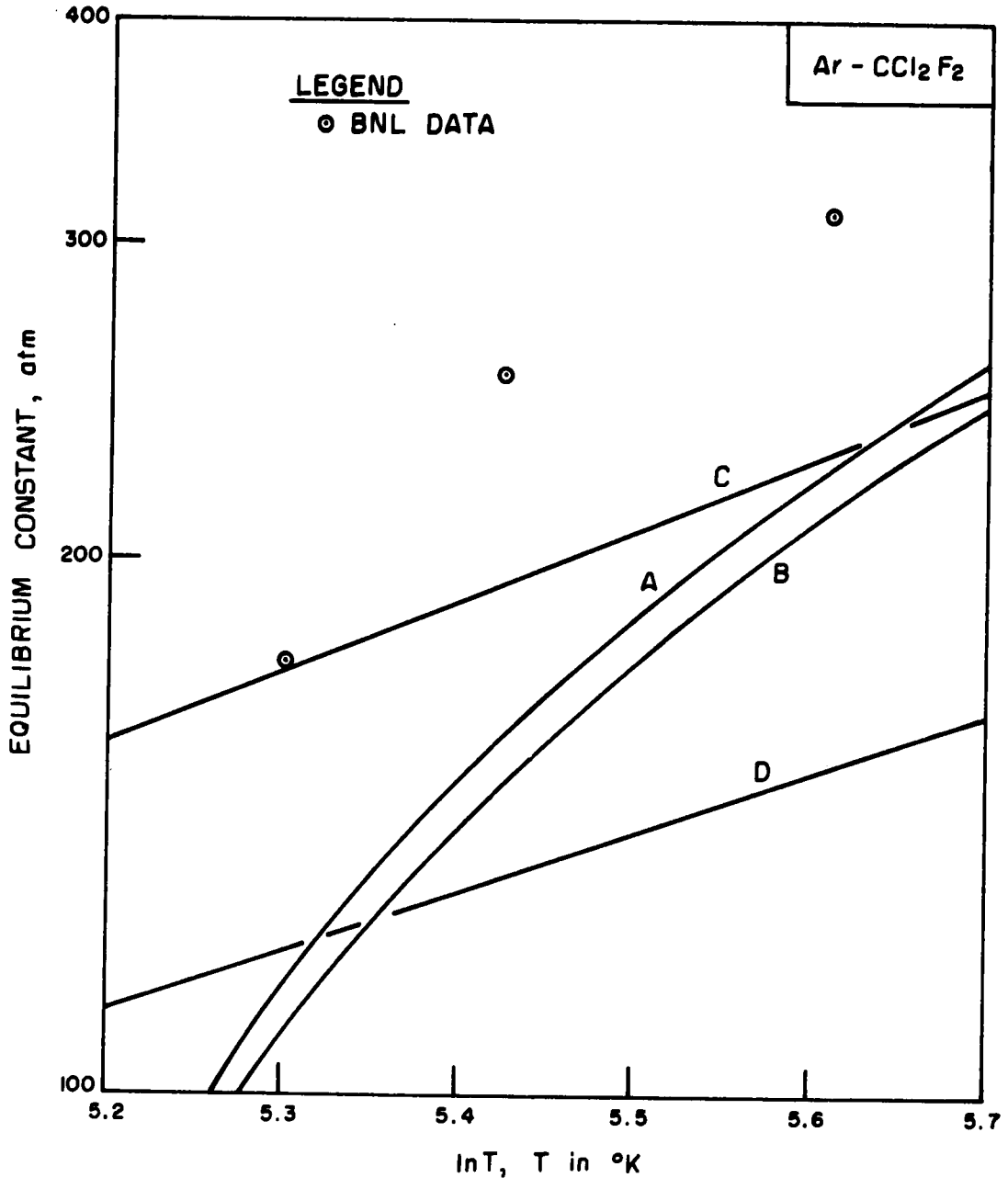


Figure 7. Predicted Equilibrium Constants for Ar in CCl_2F_2. Curve "A" is based on the regular solution equations with Prausnitz and Shair's solubility parameters. Curve "B" is based on the same equations with Yen and McKetta's solubility parameters. Curve "C" is based on $C_2Cl_3F_3$ behavior. Curve "D" is based on perfluoro-solvent behavior.

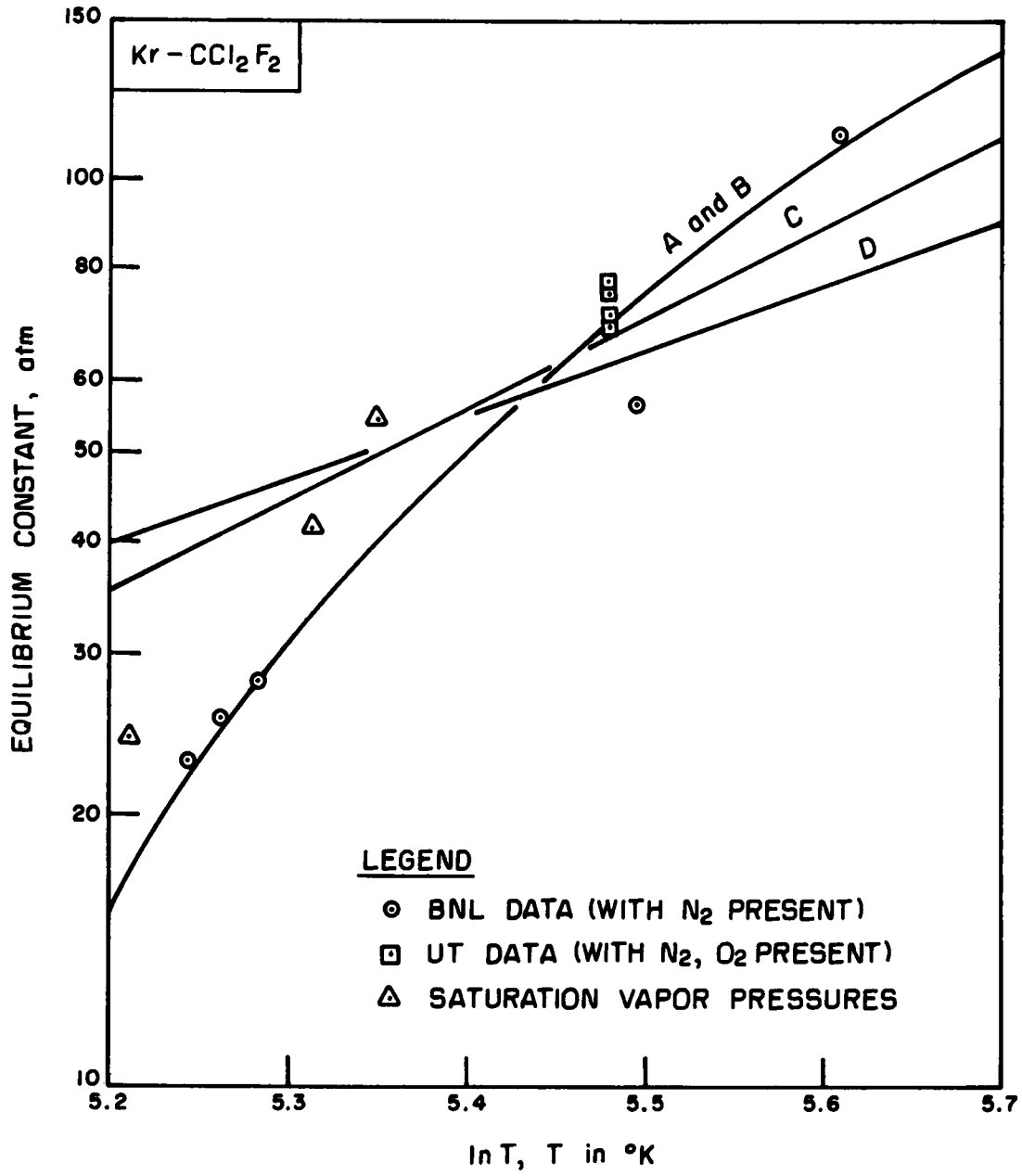


Figure 8. Predicted Equilibrium Constants for Kr in CCl_2F_2. Curve "A" is based on the regular solution equations with Prausnitz and Shair's solubility parameters. Curve "B" is based on the same equations with Yen and McKetta's solubility parameters. Curve "C" is based on $C_2Cl_3F_3$ behavior. Curve "D" is based on perfluoro-solvent behavior.

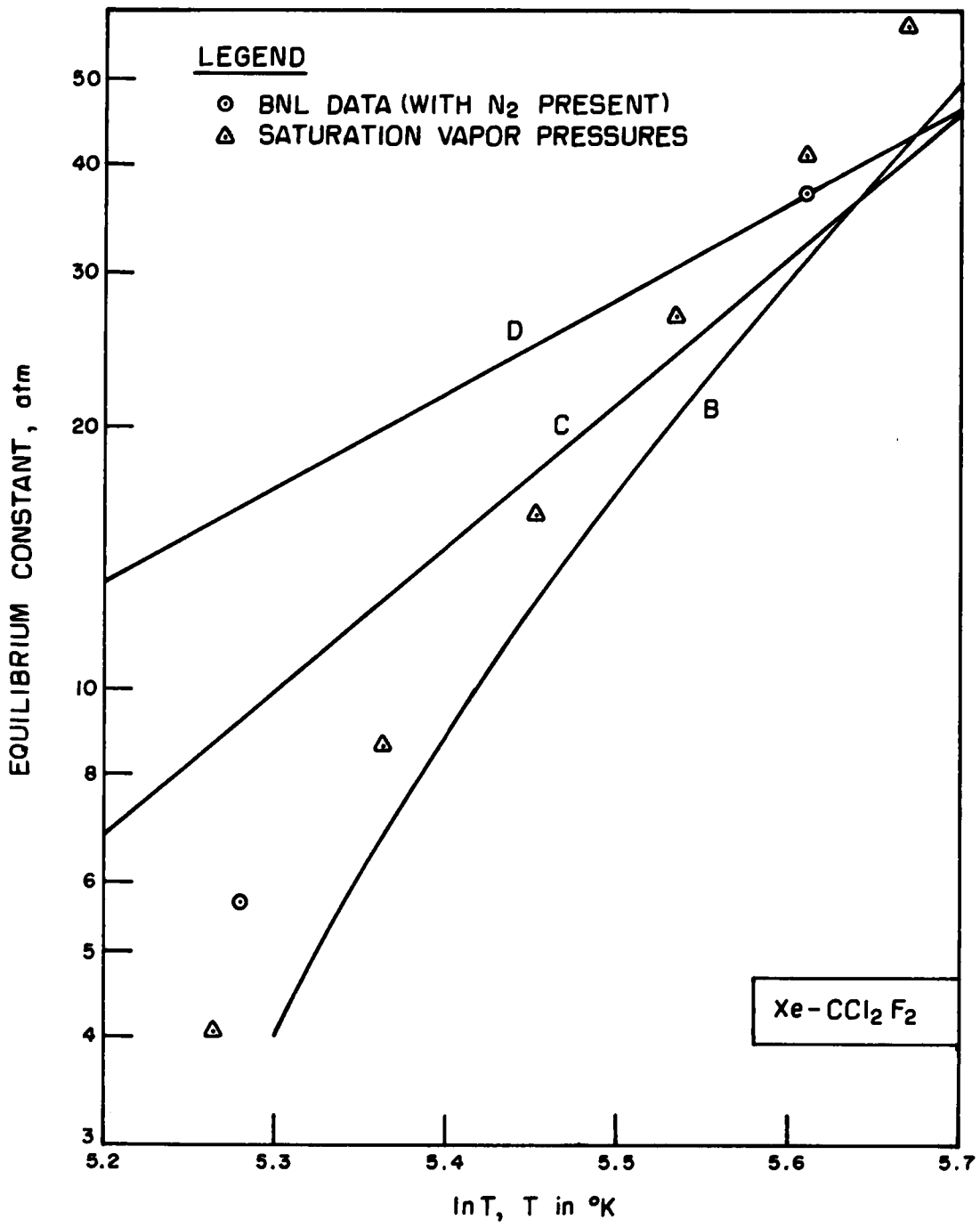


Figure 9. Predicted Equilibrium Constants for Xe in CCl_2F_2. Curve "B" is based on the regular solution equations with Yen and McKetta's solubility parameters. Curve "C" is based on $C_2Cl_3F_3$ behavior. Curve "D" is based on perfluoro-solvent behavior.

those figures ranging from about 5.35 to 5.52. While it might be tempting to argue for or against one predictive technique or another, the decision was made here, for He, N_2, O_2, and Ar, to choose the equilibrium constants over this narrow temperature range midway in the regions of the values predicted by the various techniques used. For Kr, the agreement between the regular solution curve and the reported data was too enticing to overlook, so this curve was linearized over the range of -80 to -10°F. Finally, for Xe, the two reported solubility data points were relatively close to the saturation vapor pressure line, for which more data were available, so that the vapor pressures were selected as the basis in this case.

In reviewing all the above information on reported and estimated equilibrium constants, it is apparent that the experimental data and the estimates are much closer for Kr and Xe than for the carrier gases. This could well be due to the fact that the experimental measurements for the Kr and Xe were made at low partial pressures and used radioactive tracers to improve the analytical accuracy.

In Table XIV, correlating constants are presented which give the selected binary equilibrium constants related to 1 atm partial pressure in the range of -80 to -10°F using equation (28), but with T_1 = 249.6°K. Also included in the table are summaries of the variations between the selected numbers and the outer boundaries of all those values estimated using the various techniques. Based on these outer boundaries, the selected constants are within ±25 percent for He and ±20 percent for N_2, O_2, and Ar over the temperature range of interest. Similarly, if one believes, after examination of Figures 4 through 9, that the

TABLE XIV

Selected Binary Equilibrium Constants for Gases in CCl_2F_2[a,b]

Gas	$(K_1^*)_1$, atm	β	Variances	
			Case I[c]	Case II[d]
He	1675	-2.13	±25%	-
N_2	290	0.508	±20%	±5%
O_2	182	1.52	±20%	±10%
Ar	177	0.876	±20%	+20, -0%
Kr	81.0	4.22		
Xe	24.2	6.70		

[a]Values are for use in equation (28) but with T_1 = 249.6°K.

[b]Recommended for use only in the temperature range of -80 to -10°F.

[c]Relative to extreme limits of all predicted values.

[d]Relative to limits based only on $C_2Cl_3F_3$ behavior and the regular solution theory with Yen and McKetta's parameters.

estimates based on the regular solution equations with Yen and McKetta's parameters and on the behavior of $C_2Cl_3F_3$ are better than the other two sets of estimates, then the selected constants are within 10 percent of the preferred region. Similar analyses were not made for Kr and Xe, since the evidence is that the selected parameters are substantially accurate.

After choosing the binary equilibrium constants, the N_2 estimates were tested for thermodynamic consistency using the same test applied to the experimental data for N_2. This yielded an $A_1 + A_2$ value of -4.33 versus an A_3 of -4.40. Comparison of this result with the result for the reported data, given on page 24, strongly suggests that the selected constants are considerably more consistent.

To sum up, the binary equilibrium values assumed for this work for the various gases in CCl_2F_2 between temperatures of -80 and -10°F are shown in Figure 10. It should be remembered that to apply these binary data, which are related to 1 atm, at other pressures and with other components present formally requires the adjustments presented previously.

Based on the above analysis, it can also be suggested that CCl_2F_2 would be an excellent solvent for further experimental and theoretical investigations of gas solubilities. Because of its unusual solubility parameters, CCl_2F_2 data should shed light on the perplexing perfluoro solvent anomalies.

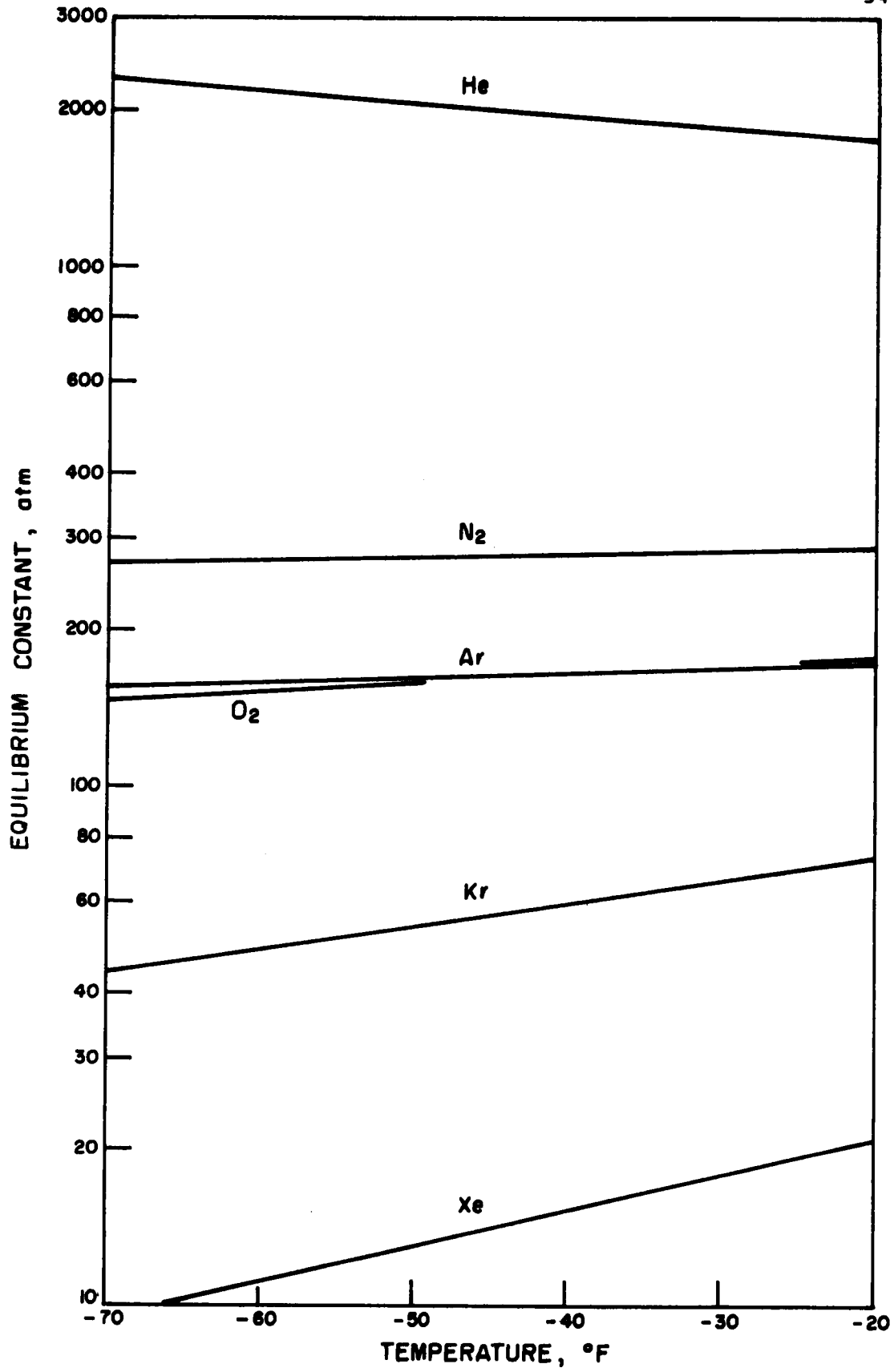


Figure 10. Selected Equilibrium Constants for Various Gases in CCl_2F_2.

CHAPTER III

EXPERIMENTAL APPARATUS AND TEST RESULTS

I. ABSORPTION SYSTEM DESIGN

The mass-transfer experiments were conducted in a pilot plant facility designed to evaluate the feasibility of the selective absorption scheme for Kr-Xe collection. Since extensive details of the facility design and hardware have been published elsewhere, only a general overview will be provided here (Merriman and Pashley, 1968; Stephenson, et al., 1970).

Pilot Plant Process Description

A schematic diagram of the test system is given in Figure 11. The major equipment items in the process were three packed columns which functioned as intimate gas-liquid contactors. The absorption section of the process consisted of a single packed column. The other two columns, each fitted with a reboiler, a flash drum, and an overhead condenser system, comprised the fractionator and stripper sections. The remainder of the process equipment included gas and solvent heat exchange and refrigeration systems, desiccant traps, a gas compressor, a solvent pump, and solvent storage tanks.

The feed gas for the absorption tests ordinarily consisted of a bulk carrier gas containing trace levels of Kr and Xe. The separation of Kr and Xe from the carrier was accomplished in the absorber, which was typically operated near 25 atm and -25°F. In the absorber, the

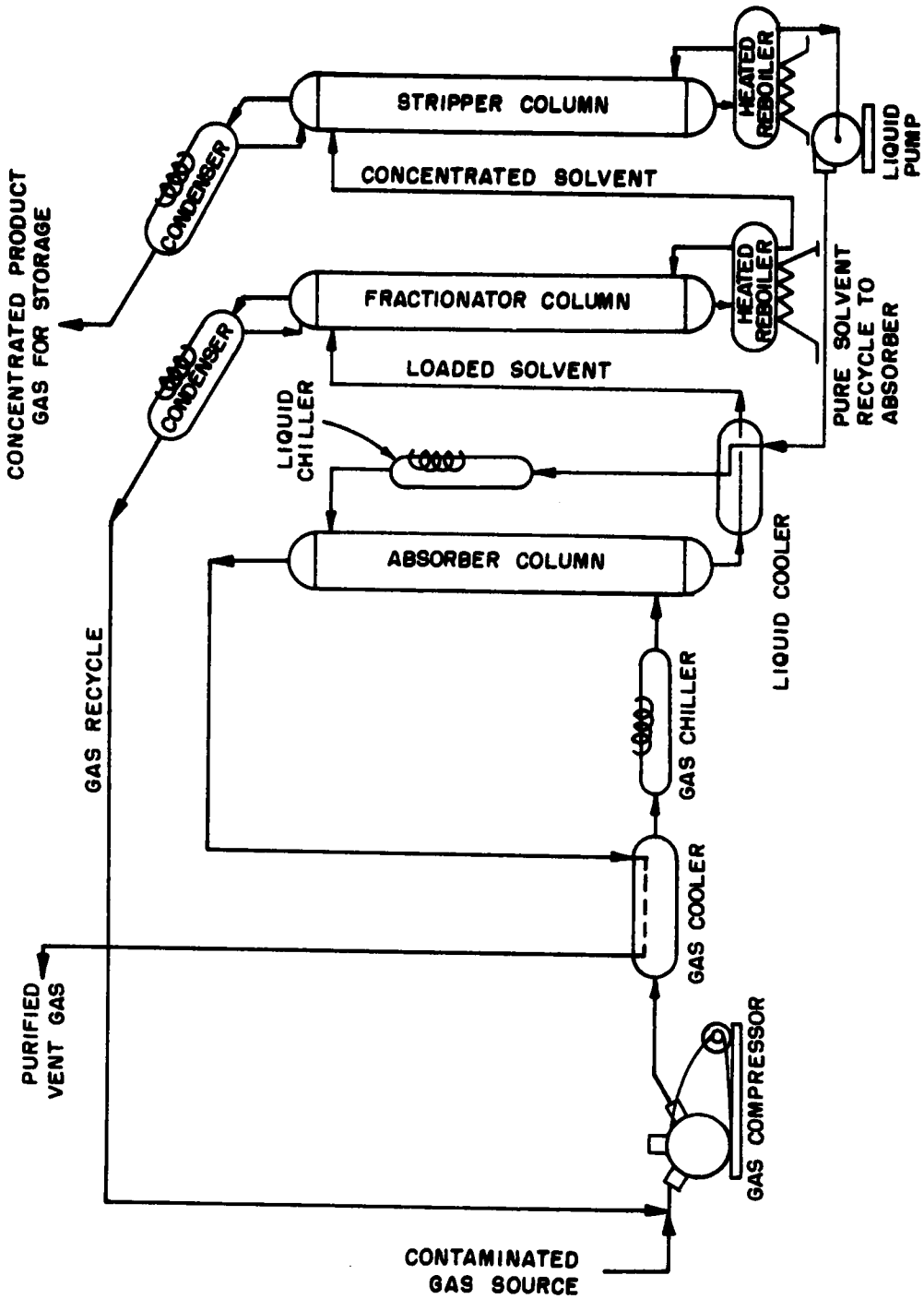


Figure 11. Krypton-Xenon Absorption Process Pilot Plant Schematic Flow Diagram.

feed, after being compressed and cooled, was contacted with downflowing solvent, resulting in essentially quantitative dissolution of the noble gas along with significant coabsorption of carrier gas. Unabsorbed carrier was vented or, as a convenience, recycled for feed makeup.

Loaded solvent from the absorber was passed to the fractionator system. The purpose of this unit was to strip the bulk of the coabsorbed carrier from the liquid stream, leaving the remaining dissolved gas more enriched in Kr and Xe. The fractionator was customarily operated at 3 atm and +33°F, and reboiled solvent vapor was used as the stripping medium. Operation of the fractionator to achieve nearly complete desorption of carrier resulted in simultaneous desorption of measurable amounts of Kr and Xe. Consequently, the fractionator off-gas was recycled to the absorption unit.

The enriched solvent stream from the fractionator was fed to the final stripper system, which was operated near 1.5 atm and 0°F. Here, virtually complete desorption of Kr and Xe was effected, again using solvent vapor from the reboiler. The stripper off-gas, concentrated Kr and Xe, represented the process product, and the solvent leaving the stripper reboiler was pumped back to the absorber column after suitable cooling.

In these pilot plant experiments, temperatures and pressures were measured using conventional instrumentation calibrated on a regular basis and replicated sufficiently through the system to provide cross-checking of data. Gas flows were measured with mass-flow meters which were also strategically located and calibrated against very accurate primary standards. Liquid flow rates were originally based on the

micrometer setting of the positive displacement-type solvent pump, but these data were later corrected on the basis of actual volumetric measurements. Concentrations were measured using a chromatograph or, in the case of trace quantities of Kr or Xe, radiation detection equipment.

Absorber Column Design

Since the data considered in the author's work are primarily associated with the absorption operation, a brief description of the absorber column is appropriate. This unit was 3 inches in diameter and approximately 10 feet long. Divided into three sections, the stainless-steel column contained approximately 7.5 feet of packing. The packing material used in the tests was Goodloe packing, which is a knitted wire-mesh type of packing rolled into 6-inch long cartridges having the desired diameter. This material was originally selected on the basis of its high efficiencies, yet relatively high throughputs, in distillation operations. Furthermore, distillation data with this packing had reportedly been successfully extrapolated from small-diameter test columns to commercial units several feet in diameter (Bragg, 1972). The Goodloe packing employed in this work was Monel and had a specific surface near 600 ft^2/ft^3 and a void fraction of 0.95.

II. EXPERIMENTAL DATA

Over the course of the ORGDP selective absorption test program, more than 150 experiments have been completed. Many of these were aimed at specific demonstration of certain features of the process, such as tolerance for various impurities, or at evaluation of possible

alternative solvents, such as CO_2 or CCl_3F. This dissertation is primarily based on a sequence of some 35 independent tests for which the data have not been previously reported and in which various pure or mixed bulk gases were combined with radioactive Kr or Xe to provide feed to the absorber. The solvent employed was CCl_2F_2. Some of the tests were replications of previous experiments in this sequence. In these cases, the parameters for the different runs were very close to each other, so they were averaged to represent a single test series at the given conditions. The data from these test series are summarized in Table XV. To illustrate the run-to-run variations typical of the repeated experiments, for the three runs of test series 2, the three feed gas flow rates were 6.93, 6.93, and 7.13 scfm, respectively.

TABLE XV

Summary of Experimental Data

Test Series	Number of Tests	Carrier Gas	Dilute Gas	Absorption Conditions T, °F	P, atm	Solvent Flow, gpm	Feed Gas Flow, scfm	Gas Absorbed, scfm	Dilute Gas Concentration Inlet, $y \times 10^9$	Inlet/Outlet
1	1	N_2	Kr	-30.0	21.4	1.3	8.83	2.51	80.5	108
2	3	N_2	Kr	-26.3	21.4	1.3	7.00	2.70	319	260
3	1	N_2	Kr	-26.0	21.4	1.3	4.95	2.57	360	494
4	1	N_2	Kr	-27.0	25.4	1.3	8.81	3.08	73.9	349
5	2	N_2	Kr	-24.5	25.4	1.3	6.93	3.32	778	408
6	3	N_2	Kr	-25.3	25.4	1.3	4.98	3.42	671	614
7	3	N_2	Kr	-30.3	25.4	0.98	7.00	2.50	500	447
8	3	N_2	Kr	-23.7	25.4	0.98	3.56	2.21	880	859
9	1	N_2	Kr	-35.0	27.9	1.3	7.62	3.32	88.5	361
10	1	N_2	Kr	-27.0	28.7	1.3	6.90	3.69	218	321
11	3	Ar	Kr	-24.0	25.4	1.3	9.72	6.04	765	112
12	3	Ar	Kr	-25.0	25.4	1.3	7.17	5.99	264	233
13	1	He	Kr	-30.0	25.4	1.3	7.29	0.74	129	219
14	3	He	Kr	-28.7	25.4	1.3	2.83	0.74	282	632
15	2	Air	Kr	-25.5	25.4	1.3	5.94	3.80	130	280
16	2	Air	Kr	-25.5	25.4	1.3	4.95	3.61	55	320
17	2	Air	Xe	-28.5	25.4	1.3	5.15	3.50	7.80	4480

CHAPTER IV

ANALYTICAL PROCEDURES

I. INTRODUCTION

The approach taken in the analysis of the experimental data was to utilize the film theory framework and sequentially apply it to the following increasingly complex mass-transfer situations;

1. The simple case where a single carrier gas (N_2, Ar or He), was absorbed in CCl_2F_2. In this case, the essential absence of additional components physically precluded any gas film, in the mass-transfer sense, providing a unique opportunity for direct calculation of liquid film mass-transfer coefficients.
2. The simple case where a very soluble gas (Kr or Xe), present in the carrier at extremely low mole fractions ($<10^{-6}$), was absorbed in CCl_2F_2 by diffusive transfer only.
3. The elementary multicomponent case, which involved simultaneous absorption of both the dilute component and a single carrier gas. This case provided an opportunity to evaluate the relationship between dilute gas mass-transfer and carrier gas coabsorption.
4. The more complex multicomponent case, which involved a mixed carrier gas (air) and a dilute, soluble species (Kr). This case provided an opportunity to investigate interferences between carrier constituents during the transfer process.

It can be seen that the combinations just described offered a fairly wide range for extending film theory concepts to absorption systems having coabsorbing carrier gases.

II. GOVERNING EQUATIONS

The basic design equations for gas absorption in packed columns are:

$$d(Gy) = K_g aSP(y - y^*)dz \ , \tag{29}$$

and

$$d(Lx) = K_L aS\rho_M(x^* - x)dz \ , \tag{30}$$

where G = gas flow rate, lb moles/hr,

L = liquid flow rate, lb moles/hr,

S = cross-sectional area of column, ft^2,

P = pressure, atm,

ρ_M = liquid molar density, moles/ft^3,

dz = increment of column length, ft,

a = packing specific surface, ft^2/ft^3,

y = bulk gas-phase mole fraction of the considered species,

x = bulk liquid-phase mole fraction of the considered species,

x^*, y^* = equilibrium bulk phase concentrations,

$K_g a$ = overall gas-phase-based mass-transfer coefficient, moles/hr-ft^3-atm, and

$K_L a$ = overall liquid-phase-based mass-transfer coefficient, moles/hr-ft^3-(mole/ft^3).

The above equations simply relate the rate of mass-transfer as the product of a transfer coefficient, a transfer area, and a concentration

gradient driving force. It is further assumed that these values are independent. In practice, of course, the transfer area is an elusive parameter, leading to frequent combination of this factor into the transfer coefficient.

When the driving forces are based instead on "interface" conditions, the corresponding equations lead to:

$$k_g aSP(y - y_i^*) = k_L aS\rho_M(x_i^* - x) \ , \tag{31}$$

where $k_g a, k_L a$ = individual gas and liquid film coefficients, and
y_i^*, x_i^* = equilibrium concentrations at the interface.

Equation (31) is based on the assumption of steady-state transfer through the two films.

Combination of the above equations leads to the following familiar relationships between the various mass-transfer coefficients:

$$\frac{1}{K_g a} = \frac{1}{k_g a} + \frac{K_i^*}{\rho_M k_L a} \ , \tag{32}$$

$$\frac{1}{K_L a} = \frac{1}{k_L a} + \frac{\rho_M}{K_i^* k_g a} \ , \tag{33}$$

and

$$K_g a = \frac{\rho_M K_L a}{K_i^*} \ , \tag{34}$$

where K_i^* = equilibrium constant, atm.

Direct determination of individual film coefficients has proved difficult, and these values are usually deduced by cross-correlating overall data or by neglecting the resistance to transfer offered by one

film or the other. Generally speaking, in absorption systems where the equilibrium constant is very large (>10,000 atm), the overall coefficient is dominated by the liquid terms. Conversely, when the gas is very soluble (K_i^*<100 atm), the gas terms are more significant. Since these two extremes represent many systems of commercial importance, and because the analytical techniques can be greatly simplified in these cases, the region of moderate solubility has been relatively unreported. This is particularly true in the sense of direct, as opposed to inferential, measurement of individual coefficients.

III. SUMMARY OF CALCULATIONAL PROCEDURES

The specific equations used in the analysis of the carrier gas, dilute gas, and combined transfer data are presented in subsequent chapters dealing more completely with these topics. Also, the calculation procedures are detailed in the Appendix. However, a summary of the procedures at this point will introduce how the various mass-transfer data were obtained.

In the case of absorption of a pure carrier gas, equation (30) can be integrated explicitly to obtain both overall and liquid film coefficients, which are equal in this instance. Analysis of the He data proved to be an exception, since this gas apparently approached saturation in the 7.5-foot tall absorber. Consequently, He coefficients were estimated by extrapolation. The resulting mass-transfer coefficients for the carriers were used together with material balance relationships to establish the gas and liquid flow rates and liquid concentrations at various increments in the column. These calculations

required iterative procedures, but convergence proved rapid using the Newton-Raphson method.

Next, two different overall gas-phase mass-transfer coefficients were calculated for the dilute gas. This required numerical solution of the appropriate forms of equation (29), using the incremental column data previously calculated in the analysis of the liquid-phase transfer of the carrier component. For these calculations, a Runge-Kutta scheme was employed, after which additional incremental points for the dilute gas concentrations were obtained from the material balance equations.

To illustrate the results of the various calculations, profiles for some typical experiments are illustrated in Figures 12 and 13. The surprisingly high solubility of carrier gases in CCl_2F_2 is again reflected here. Because of this solubility, the change in gas flow rate between the column inlet and the column exit is appreciable.

IV. SOME ADDITIONAL DEFINITIONS

Frequently, absorption problems are presented in terms of soluble species contained in a stagnant carrier to be absorbed in a solvent. As noted previously, the most distinguishing feature of this project is the presence of a nonstagnant carrier, to use the analogous language. Because the word "stagnant" has hydrodynamic connotations, its use somewhat obscures the real intent of the problem statement given above. As a result, for this dissertation, the distinction will be made in terms of soluble versus insoluble carrier gases. The methods developed in the following chapters are intended to be used for systems having soluble, coabsorbing carrier gases; they can also be applied to simpler

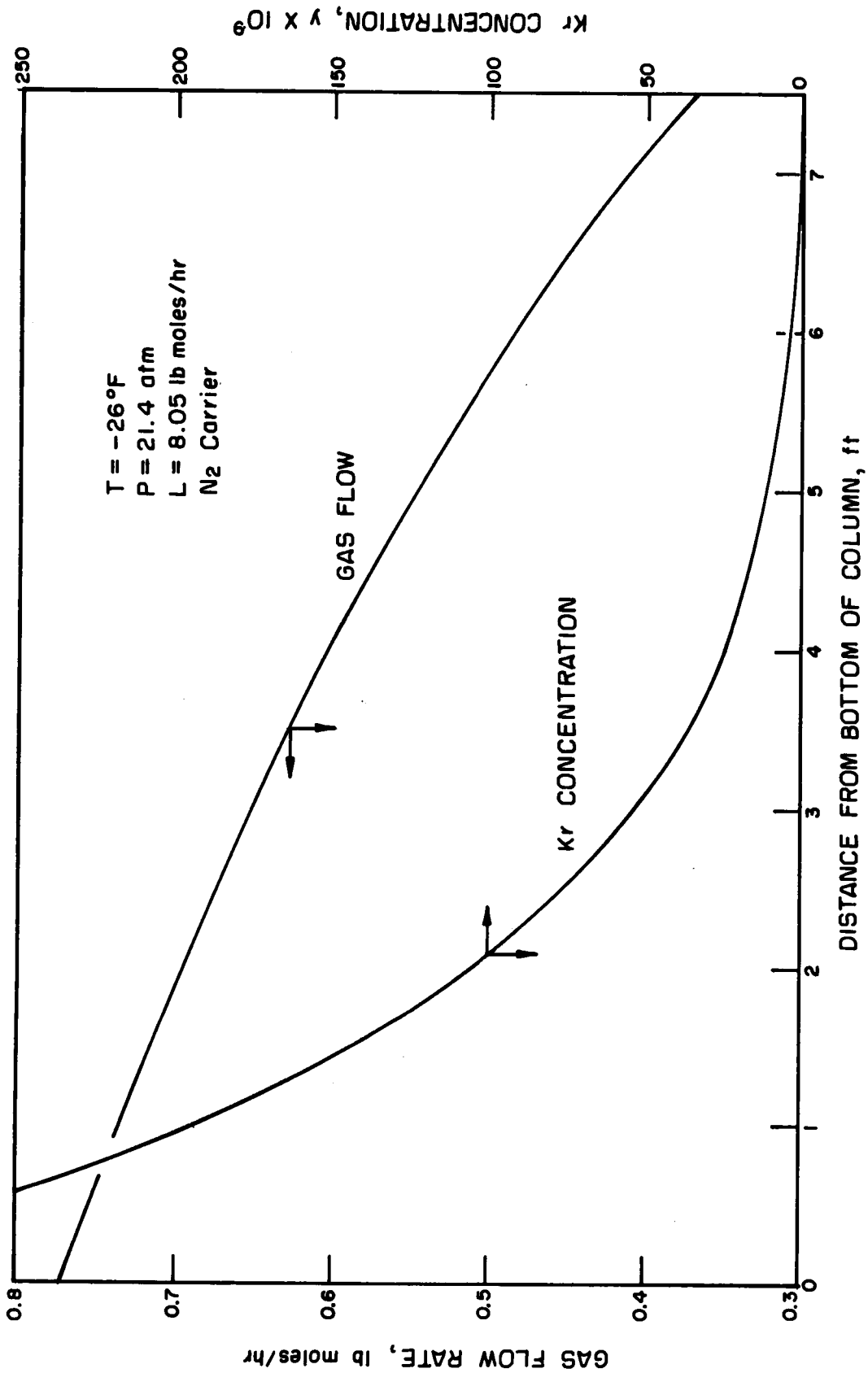


Figure 12. Profile Data for Test Series 3. These profiles are calculated.

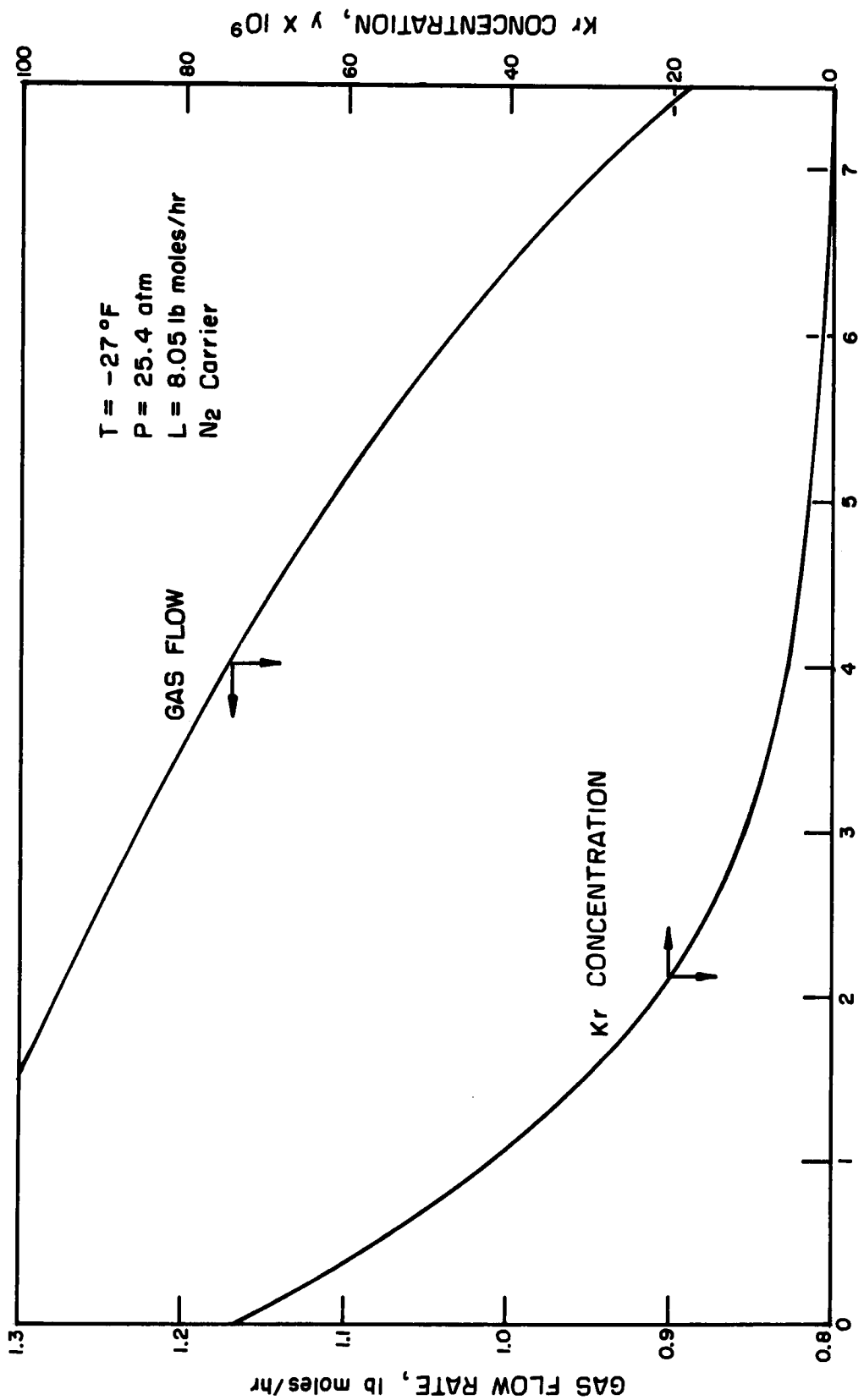


Figure 13. Profile Data for Test Series 4. These profiles are calculated.

problems, but the extra computational work is unnecessary. Other, more conventional, methods are intended to be used for systems having insoluble carrier gases.

The immediate question is: What, quantitatively, is the demarcation between soluble and insoluble carriers? While it is not possible to provide an absolute answer applicable to all absorption problems, it appears reasonable, based on this work, to suggest that carriers having K_i^* values above 10,000 atm can be considered insoluble, below 1,000 atm as soluble, and in-between as moderately soluble. This is to say that for systems with insoluble carriers, such as air-water systems, the conventional design approaches are applicable; for systems with soluble carriers, such as N_2-CCl_2F_2 systems, the procedures developed in this dissertation should be used to avoid substantial error and compromise of the problem; and for systems with moderately soluble carriers, such as He-CCl_2F_2 systems, either set of design procedures could probably be used, based on the designer's judgment and the specific location of K_i^* in the 1,000-to-10,000 atm range.

CHAPTER V

CARRIER GAS MASS-TRANSFER DATA

I. INTRODUCTION

As noted in the previous chapter, the tests involving absorption of a single carrier gas afforded a unique opportunity for direct calculation of liquid film mass-transfer coefficients. In these tests, the concentrations of the dilute gas in the carrier were in the range of 10^{-9} to 10^{-6} mole fraction. Thus, the assumption of a constant carrier gas concentration throughout the column equal to unity was very sound. In such a situation, the carrier gas concentration at the gas-liquid interface almost exactly equals its concentration in the bulk gas stream. Consequently, there is virtually no diffusive driving force for carrier transfer between the bulk of the gas stream and the interface and, therefore, no gas film for the carrier in the mass-transfer sense. It is emphasized that this is not to say that there is no gas film in the hydrodynamic sense. Rather, whatever laminar or other film there might be, there is essentially no carrier gas concentration gradient across it.

Having an interfacial carrier gas concentration of one obviously simplified the analysis of the absorption data for those tests involving essentially pure carriers. Equation (30), page 62, could be integrated directly, since the equilibrium value, x^*, was constant throughout the column at $1/m$. Here, m is the equilibrium constant, $K_i^*/\eta_i P$, where η_i is the fugacity coefficient. The result of the integration

depends on what assumption one makes regarding the variation of $K_L a$ with the liquid flow rate in the column. In the case of the liquid data, the variation of the liquid flow from the top of the column to the bottom was relatively slight, making it practically inconsequential as to what variation was in fact assumed. Although the data were processed using assumed variations of $K_L a$ with L ranging from L^0 to L^1, there was so little difference in the results that the constant $K_L a$ numbers were chosen. In this situation, the integrated form of equation (30) is:

$$\frac{K_L a \rho_M S Z}{L_2} = \frac{1}{1 - x^*} \left[\frac{1}{1 - x^*} \ln \left(\frac{x^*(1 - x_1)}{x^* - x_1} \right) - \frac{x_1}{1 - x_1} \right], \qquad (35)$$

where L_2 = pure solvent flow rate, lb moles/hr, and

x_1 = concentration of component in the exit liquid.

Equation (35) was used in the analysis of all the pure carrier gas data except that for He. It appeared that He approached saturation in the column. When saturation occurs, the corresponding $K_L a$ from equation (35) is indeterminate, and the physical analysis of rate constants is obscured by mathematical realities.[2] As long as there is a fair difference between actual and saturation concentrations, errors in experimental and equilibrium data and their impact on $K_L a$ are of corresponding magnitude, as will be illustrated in a subsequent section.

---

[2]From a practical design standpoint, of course, saturation simplifies the determination of quantities of gas which will be absorbed in a tower.

When the actual and saturation concentrations are very nearly equal, on the other hand, a 5 percent error in a measured flow can easily affect $K_L a$ by a factor of 10. Of course, this is why absorption or desorption experiments with very insoluble gases are conducted in the shortest possible test columns, considering, in addition, end effects and the analytical precision available. For these reasons, the He coefficients had to be extrapolated using the N_2 and Ar data, with difference calculations used to establish profiles.

II. MASS-TRANSFER COEFFICIENTS

The liquid-phase mass-transfer coefficients calculated or estimated for the absorption of carrier gases are listed in Table XVI, together with corresponding diffusion coefficients and Reynolds and Schmidt numbers. In this analysis, the Reynolds number is defined as:

$$Re = \frac{6W}{a\mu} , \tag{36}$$

where W [=] $lb/hr\text{-}ft^2$.

There are several forms of Reynolds numbers used for flow in packed beds. In some cases, the characteristic diameter, D_p, is simply taken as $1/a$. In other cases, D_p is calculated as the diameter of a sphere having the same surface area as a piece of packing. Since the first approach lacks somewhat in consistency with the usual idea of what a Reynolds number is, and since the second approach breaks down when nondiscreet packings, such as mesh packings, are used, an alternative was employed here. The value, $6/a$, used in equation (36), is the

TABLE XVI

Liquid-Phase Mass-Transfer Coefficients

Series	Carrier Gas	$D_L \times 10^4$, ft^2/hr	Re	Sc	K_La, hr^{-1}
1	N_2	2.4	215	40.4	27.5
2	N_2	2.5	220	38.2	31.7
3	N_2	2.5	220	38.1	29.1
4	N_2	2.5	220	38.6	29.4
5	N_2	2.5	224	37.2	33.9
6	N_2	2.5	224	37.7	35.8
7	N_2	2.4	163	40.6	24.9
8	N_2	2.5	169	36.8	20.6
9	N_2	2.3	211	43.7	27.5
10	N_2	2.5	222	38.6	32.4
11	Ar	2.8	232	33.1	40.5
12	Ar	2.8	230	33.6	39.5
13	He	3.1	211	31.0	34[a]
14	He	3.2	213	30.4	35[a]

[a]Extrapolated values.

diameter of a sphere having the same specific surface-to-volume ratio as the packing under consideration. It is suggested that this definition of D_p allows a consistent approach to the analysis of data taken using various packings.

Although the experimental data covered reasonably wide ranges of carrier gas type, gas flow rate, and pressure, the changes in those variables influencing $K_L a$ were not considered to be great enough to warrant an extensive independent correlation. Instead, it was decided to fix the relationships between $K_L a$ and "standard" correlating groups and simply determine a single correlating constant. In Table XVII, the dependencies proposed by other authors of $K_L a$ on diffusion coefficient, Reynolds number, Schmidt number, the group $(\rho_L/\mu_L g_C)$, characteristic diameter, and column height are summarized (Perry and Chilton, 1973). It is apparent that a universal correlating model for liquid-phase mass-transfer coefficients in packed beds has not been discovered. Based on a review of these and other relationships, the powers chosen for the Reynolds and Schmidt numbers were 2/3 and ±1/2, respectively. Using these selections, the experimental data were fit as follows:

$$K_L a = 560\, D_L\, Re^{2/3}\, Sc^{1/2}\ , \text{ and} \tag{37}$$

$$K_L a = 0.0164\, Re^{2/3}\, Sc^{-1/2}\, \left(\frac{\rho_L}{\mu_L g_C}\right)^{-1/3}\, (aD_p)^{0.4}\ . \tag{38}$$

Both equations (37) and (38) represent the experimental data with a standard deviation of about 11 percent. The inclusion of D_L as a correlating parameter is appealing because the mass-transfer coefficient

TABLE XVII

Summary of $K_L a$ Correlating Groups[a]

Author	Exponent of Parameter Group					
	D_L	Re	Sc	$\rho_L/\mu_L g_c$	D_p	Z
Sherwood and Holloway	1	.65-.78	0.5	0	0	0
Cornell	0	0	-0.5	0	0	0.15
Shulman, et al.	1	0.45	0.5	0	-1	0
Onda, et al.	0	0.67	-0.5	-0.33	0.4	0

[a]This table indicates the ranges of exponents appearing in correlations of $K_L a$ (or K_L) = fn (various groups).

Source: Perry and Chilton, 1973.

itself is envisioned as diffusivity divided by some characteristic film thickness. For this reason, equation (37) is preferred here and for systems involving similar components and packings.

Equation (38) was employed primarily to check the general consistency of the results with other $K_L a$ data. Reportedly, the equation has been used to fit a wide variety of transfer data for both aqueous and organic systems (Perry and Chilton, 1973). Actually, the original equation separates K_L and a, uses a different Re than in this work, and is based on more common packing materials (a's between 50 and 125) than the one used in these experiments. Adjusting the original constant, 0.0051, by multiplying by the average a on which it was based and correcting for the Re differences results in a new value of about 0.014. Thus, the value of 0.0164 in equation (38) indicates good agreement with expectations based on other mass-transfer data. In a similiar vein, Sherwood and Holloway correlated mass-transfer data using an equation very near equation (37). Their constants ranged from 80 for 2-inch rings to 280 for 1/2-inch rings (Perry and Chilton, 1973). Thus, in a qualitative sense, the constant in equation (37), 560, appears reasonable for the very high surface area packing employed here.

As a further note, many investigators have commented on the difficulty in separating K_L and a, however desirable this might be from a theoretical standpoint. In numerous examples, $K_L a$ values have been found to vary little with different packings. In some cases, effective areas have nevertheless been estimated using various techniques and then employed to determine K_L values. It seems possible that the

moderate successes of these efforts could be the result of most data being based on packings which have areas within a factor of 2 or 3 of each other.

Using the extrapolated constants for the He tests, the measured column outlet flows for these runs are matched to within about 2 percent, which is well within the experimental scatter typical of these experiments.

Finally, the data suggest a slightly higher exponent for Re than 2/3. As noted previously, however, the number of data sets did not appear to justify establishing a different value, and the end results of the correlation were satisfactory.

III. SENSITIVITY ANALYSIS

Even though the liquid-phase mass-transfer coefficients appear consistent, both internally and with respect to expected results, a sensitivity analysis was made to show the influence of changes in system and property variables on the $K_L a$ values. This was investigated because the carrier gas coefficients become very important in the subsequent analysis of the dilute gas transfer. To conclude this chapter, the results of this analysis for a typical N_2 run (series 5) are summarized in Table XVIII. There, changes in $K_L a$ resulting from perturbations of the equilibrium constant, gas flow measurements, and liquid flow measurement are listed. It is suggested that this type of analysis is helpful in illustrating key areas where the needs for good experimental numbers are most important. In this case, no single parameter emerged as being unusually sensitive.

TABLE XVIII

Summary of Sensitivity Analysis

Variable	$K_L a$, hr^{-1}, for Indicated Change in Variable				
	-25%	-10%	0%	+10%	+25%
Equilibrium Constant	20.6	27.3	33.9	39.7	54.6
Gas Absorbed	21.0	28.0	33.9	41.4	58.0
Liquid Flow Rate	50.6	37.7	33.9	31.8	29.4

CHAPTER VI

DILUTE GAS MASS-TRANSFER DATA

I. INTRODUCTION

The objective in the analysis of the dilute gas mass-transfer data was to relate the absorption of the dilute component not only to its concentration gradient driving force but also to the effects of the coabsorption of the carrier gas. It was further desired to isolate these effects so that, for the gases considered in this dissertation, Kr-Xe absorption from a given carrier gas could be generally predicted with some confidence even if direct experimental data were not available for the particular dilute component-carrier gas system of interest. The starting point for this effort was the basic packed gas absorber design equation, equation (29), repeated below:

$$d(Gy) = K_g aSP(y - y^*)dz \quad , \tag{29}$$

and the goal was identification of the appropriate form of the coefficient, $K_g a$, to be used when carrier coabsorption occurs.

Rewriting this equation in terms of a local flux (N_A), a local coefficient, and a local concentration gradient gives:

$$N_A = K_A \Delta y_A \quad . \tag{39}$$

Here, for purposes of illustration, the equation has been simplified by omitting the writing of some of the factors explicitly contained in equation (29), incorporating these instead into a general coefficient,

K_A, with different units than $K_g a$. The basic relation between the mass-transfer rate, the coefficient, and the driving force has been preserved, however. The subscript A in equation (39) is used to designate the dilute soluble component.

It can be seen that equations (29) and (39) represent the total absorption of component A, by all transfer mechanisms. In this problem, it is suggested that two factors are at work. One of these is, of course, the transfer of dilute component A due solely to its concentration gradient. This is referred to in this dissertation as the "diffusive" transfer of the dilute gas. The second factor, important when the carrier gas is soluble, is the transfer of A due to the bulk movement of the coabsorbing carrier gas, which contains A. This mechanism is referred to as the "bulk" transfer of the dilute component, and the sum of the two, accounting for all the transfer of the soluble species, is referred to as the "total" transfer. The mass-transfer coefficient, $K_g a$, as it appears in equation (29), is thus a total mass-transfer coefficient as defined here.

The bulk transfer of component A is given by:

$$N_A^B = y_A(N_A + N_B + N_C + \ldots) \ , \tag{40}$$

where the subscripts B and C on the right-hand side are used to designate carrier gas fluxes.

If the bulk transfer, equation (40), is subtracted from the total transfer, equation (39), the net result is the diffusive transfer:

$$N_A - y_A(N_A + N_B + N_C + \ldots) = K_A^* \Delta y_A \ , \tag{41}$$

where the superscript has been added in K_A^* to indicate that this is now a diffusive mass-transfer coefficient for component A. At this point, the left-hand side of equation (41) gives only the diffusive transport, and the right-hand side contains, appropriately, the diffusive transfer coefficient and the concentration gradient. The analogous equation in the form of the gas design equation is:

$$d(Gy) - ydG = K_g a^* SP(y - y^*)dz \ , \tag{42}$$

where $K_g a^*$ is the diffusive mass-transfer coefficient for the dilute gas expressed now in the customary units.

This picture, then, represents the transfer of a dilute soluble species as the usual diffusive transfer superimposed on a net flux caused by the coabsorption of the soluble carrier. In this case, the mass-transfer of a component in a multicomponent system is viewed as not necessarily being directly proportional to, or strictly dependent on, its concentration gradient. In the more conventional problem, with an insoluble carrier, the carrier gas flow rate is essentially constant. When all the soluble species in that particular case are also present at very low concentrations, dG is essentially zero, and equations (42) and (29) become identical. Even when the soluble component concentrations are too high to justify the assumption of a constant gas flow rate, the concentrations and the design equations can be rewritten in terms of mole ratios based on the insoluble carrier gas rate, G_S, and the ensuing dG_S vanishes. The point is that no distinction between diffusive, bulk, and total dilute gas mass-transfer is required when

the carrier gas does not coabsorb, and more straightforward approaches than the one considered in this chapter are possible.

A specific purpose of the type of analysis undertaken in this chapter was to provide a more realistic framework for processing and correlating the experimental mass-transfer data for systems having coabsorbing carrier gases. This should improve the confidence with which design calculations can be made for these systems. A more general purpose, however, was to provide, within the overall limitations of the various gases and parameters considered in this dissertation, a more rational way to extend the results of the work to the prediction of dilute gas transfer in dilute gas-carrier gas systems for which direct test data might not be available. The basic ingredients of such an analysis are a general accounting of carrier gas coabsorption, such as that given in the previous chapter; a general description of dilute component transfer from which the carrier effects have been separated; and an overall relationship between the two dilute gas transfer modes which can be applied to the specific cases of interest.

II. EXPERIMENTAL DATA REDUCTION

The first step in the treatment of the dilute gas data was to retrieve the two mass-transfer coefficients, i.e., the total coefficient, $K_g a$, and the diffusive coefficient, $K_g a^*$.[3] Equation (29) was integrated to obtain $K_g a$, and equation (42) was integrated to obtain $K_g a^*$.

---

[3]Because of the way in which the concentration gradients have been expressed, these are also overall coefficients.

As discussed in the Appendix, both integrations were numerical. The resulting transfer coefficients are listed in Table XIX, along with other parameters.

III. DIFFUSIVE TRANSFER DATA

Prior to correlating the diffusive mass-transfer coefficients for the dilute gases, correlating groups used by others for this kind of data were again reviewed. Table XX summarizes some of the dependencies of $K_g a$ data on various parameters employed for other systems (Perry and Chilton, 1973). No universal form has been found, as was the case for the liquid film coefficients for the carrier gases. In fact, it has been stated that there is more variation from system-to-system between gas-phase correlating forms than there is for liquid-phase correlations (Perry and Chilton, 1973). In this project, therefore, two forms were chosen to correlate the diffusive mass-transfer coefficients.

The first correlation includes several factors used by other investigators (Perry and Chilton, 1973):

$$K_g a^* = C D_{AB} \, Re^{1.25} Sc^{0.33} / T \, , \qquad (43)$$

where $K_g a^*$ [=] lb moles/hr-ft^3-atm,

T [=] °R, and

D_{AB} [=] ft^2/hr.

Values of the constant, C, for each carrier gas were 95.5 for He, 28.7 for N_2, 20.1 for air, and 19.1 for Ar.

TABLE XIX

Dilute Component Gas-Phase Mass-Transfer Coefficients

Series	D_{AB}, ft^2/hr	Sc	Re[a]	P,atm	T,°R	Dilute Component Mass-Transfer Coefficients, lb moles/ft^3-hr-atm	
						Total	Diffusive
1	0.020	0.938	208	21.4	430	1.19	1.12
2	0.020	0.938	164	21.4	433	0.960	0.873
3	0.020	0.938	116	21.4	434	0.618	0.530
4	0.0171	0.938	206	25.4	433	1.11	1.03
5	0.0173	0.937	162	25.4	435	0.770	0.671
6	0.0172	0.937	116	25.4	434	0.486	0.333
7	0.0169	0.938	165	25.4	429	0.932	0.858
8	0.0174	0.937	82.9	25.4	436	0.365	0.288
9	0.0150	0.939	181	27.9	425	0.736	0.657
10	0.0151	0.938	162	28.7	433	0.601	0.508
11	0.0156	0.927	255	25.4	436	0.908	0.719
12	0.0155	0.927	188	25.4	435	0.603	0.486
13	0.0684	1.86	21.4	25.4	430	0.889	0.853
14	0.0688	1.86	8.27	25.4	431	0.323	0.279
15[b]	0.0171	0.940	139	25.4	434	0.540	0.418
16[b]	0.0171	0.940	116	25.4	434	0.418	0.277
17[b]	0.0138	1.15	121	25.4	431	0.589	0.291

[a]Based on inlet gas flow.

[b]In these tests, air was treated as if it were a single pure gas.

TABLE XX

Summary of Possible Relationships Between $K_g a$ and Various Parameters

Author	Dependance of $K_g a$ on Indicated Parameter					
	G	L	D_{AB}	Sc	Re	Other Factors Used
Sherwood and Holloway	0.69	0.33				
Cornell		0.50		-0.50		Z, μ_L, ρ_L, σ, column diameter
Onda, et al.			1	0.33	0.7	T, a, D_p

Source: Perry and Chilton, 1973.

The second correlation is a simpler empirical relationship obtained by starting with a number of parameters possibly influencing $K_g a^*$ and rejecting those which did not statistically affect the fit:

$$K_g a^* = \frac{0.71 \langle G \rangle^{1.22}}{P^{1.09}} , \tag{44}$$

where $K_g a^*$ [=] lb moles/hr-ft^3-atm,

P [=] atm, and

$\langle G \rangle$ = average gas flow rate, lb moles/hr-ft^2.

Both equations (43) and (44) fit the experimental data with a standard deviation of about 12 percent. The agreement is illustrated in Figures 14 and 15. Equation (44) has one advantage, in that it does not require a specific constant for each carrier gas. This equation does require the average gas flow rate, but this can be directly obtained using the carrier gas coefficients discussed in the previous chapter to establish gas flow profiles in the column. Alternately, it was observed in these experiments that the average gas flow rate was frequently about 80 percent of the inlet flow rate, so this provides a less laborious shortcut for making first estimates, if desired.

IV. TOTAL DILUTE GAS TRANSFER

With the preceding analysis and the thought in mind that the diffusive mass-transfer coefficient is analogous to the customary coefficient used for systems with insoluble carriers, the relationship between dilute component mass-transfer and carrier gas coabsorption can be finalized. Equation (42) can be rewritten in terms of coefficients and driving forces to yield:

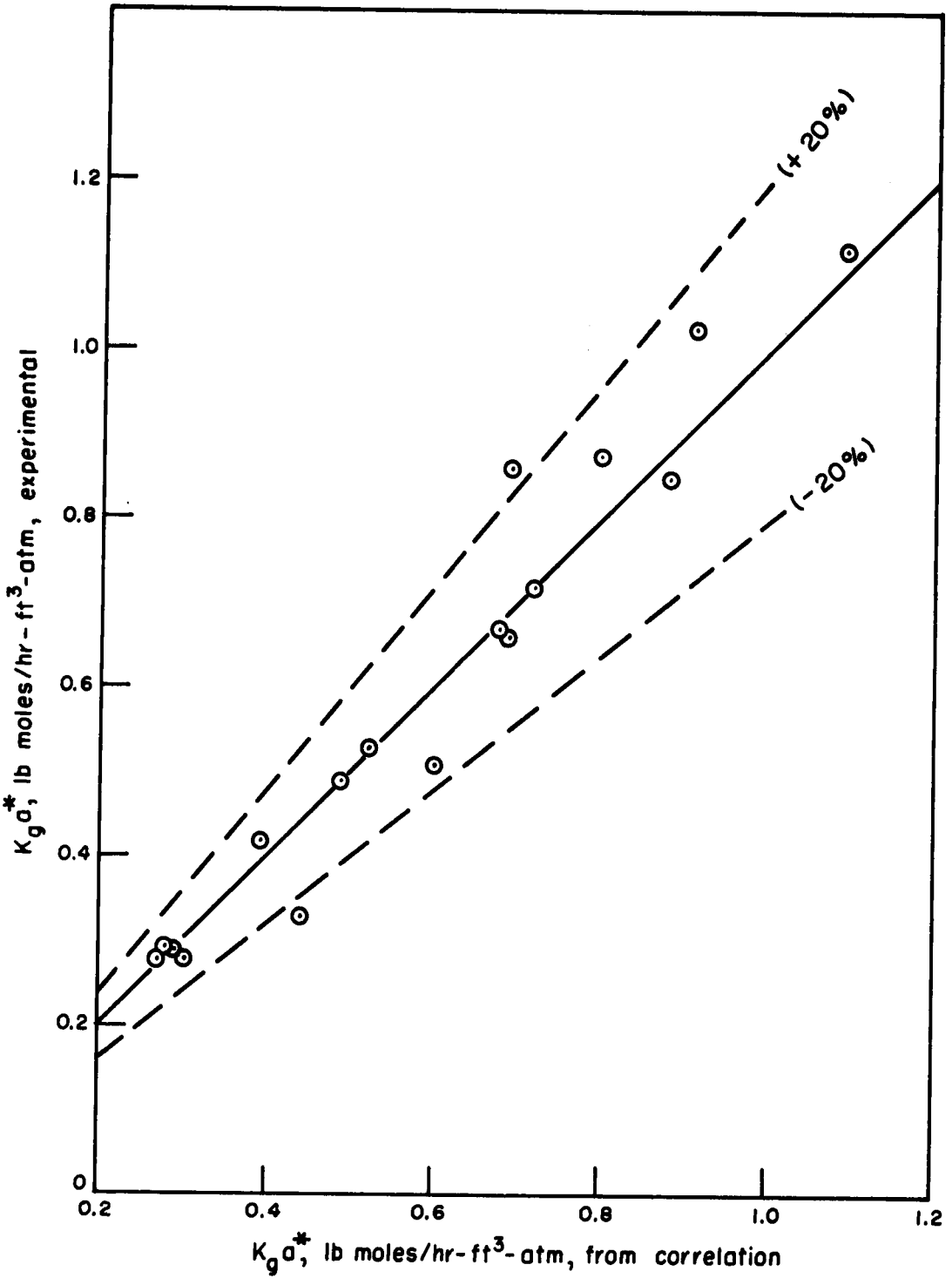


Figure 14. Comparison of Measured and Correlated Diffusive Gas-Phase Mass-Transfer Coefficients Using Equation (43).

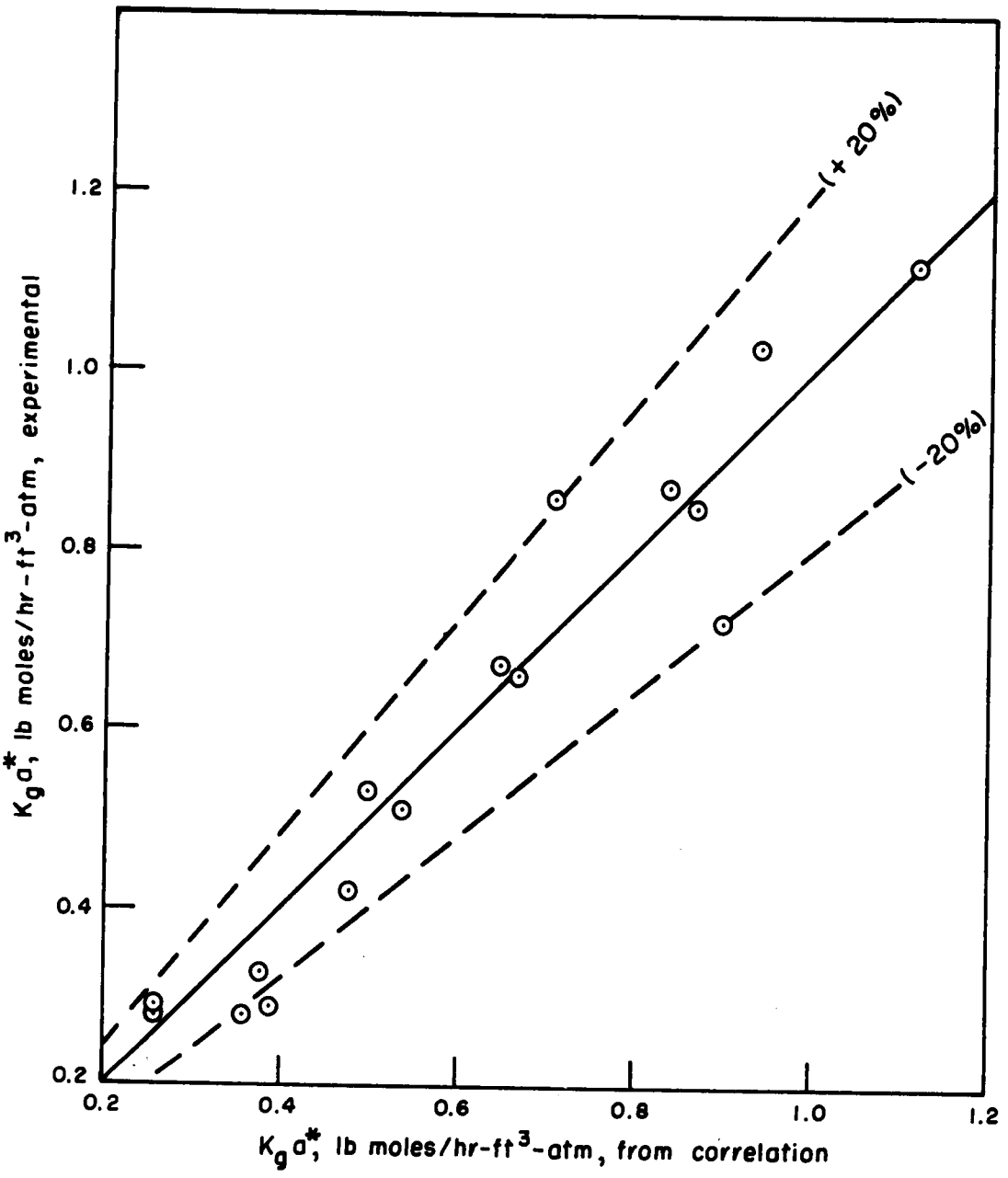


Figure 15. Comparison of Measured and Correlated Diffusive Gas-Phase Mass-Transfer Coefficients Using Equation (44).

$$K_A \Delta y_A - y_A(K_A \Delta y_A + K_B \Delta X_B) = K_A^* \Delta y_A \ , \qquad (45)$$

which provides the relationship between the diffusive and total coefficients for the dilute gas and the carrier gas coefficient. Here, only the term for a single carrier gas has been included, to simplify the presentation. Again, subscript A refers to the dilute gas and subscript B refers to the carrier gas. Some rearrangement, neglecting second-order terms, gives the following relationship between the overall mass-transfer coefficients as they have been described previously:

$$(K_g aP)_A = (K_g a^* P)_A + (K_L a \rho_M)_B \left(\frac{y_A \Delta X_B}{\Delta y_A}\right)_{avg} . \qquad (46)$$

Technically, the factor $(y_A \Delta X_B / \Delta y_A)$ should be obtained by averaging at each increment of column height. Since these data are not known at the outset of a design, however, the factor can be estimated for initial calculations by merely averaging the terminal conditions. For a binary gas mixture with essentially complete absorption of the dilute component, the average is:

$$\left(\frac{y_A \Delta X_B}{\Delta y_A}\right)_{avg} = \frac{1}{2m_B}\left(1 + \frac{L_2 + G_D - m_B G_D}{L_2 + G_D - m_A G_1}\right) , \qquad (47)$$

where L_2 = inlet solvent flow, lb moles/hr,

G_D = amount of carrier gas dissolved, lb moles/hr,

G_1 = inlet gas flow rate, lb moles/hr, and

m_A, m_B = equilibrium coefficients for dilute component A and carrier gas B, respectively.

The relationship given in equation (46) was tested as follows: First, the $K_g a^*$ values for each experiment were available from the treatment discussed in the previous section. Second, the liquid-phase transfer coefficients for the carrier gases were available from the treatment presented in Chapter V. Next, equation (47) was used to estimate the concentration gradient factor. These numbers were then inserted into the right-hand side of equation (46), and the resulting $K_g a$ was determined. These results were finally compared with the $K_g a$ values obtained through direct reduction of the experimental data using equation (29). As shown in Figure 16, the comparison proved to be very good, indicating that this view of the relationship between dilute gas absorption and carrier gas coabsorption is applicable to and internally consistent for this problem.

The basic gas-phase and liquid-phase design equations for packed absorbers were first presented in Chapter IV. The test just described also illustrates the heart of the design approach for the systems considered in this dissertation. The $K_L a$ correlations given in Chapter V can be used to characterize the carrier gas coabsorption and to provide numbers which can also be used with the liquid-phase design equation to calculate the behavior of the carrier in the absorber. The $K_g a^*$ correlations given in this chapter yield a description of dilute gas absorption by diffusive transfer but do not account for its bulk transfer. Equation (46) ties everything together for a specified carrier gas-dilute gas pair by providing $K_g a$ values which can then be used with the familiar gas-phase design equation to calculate the

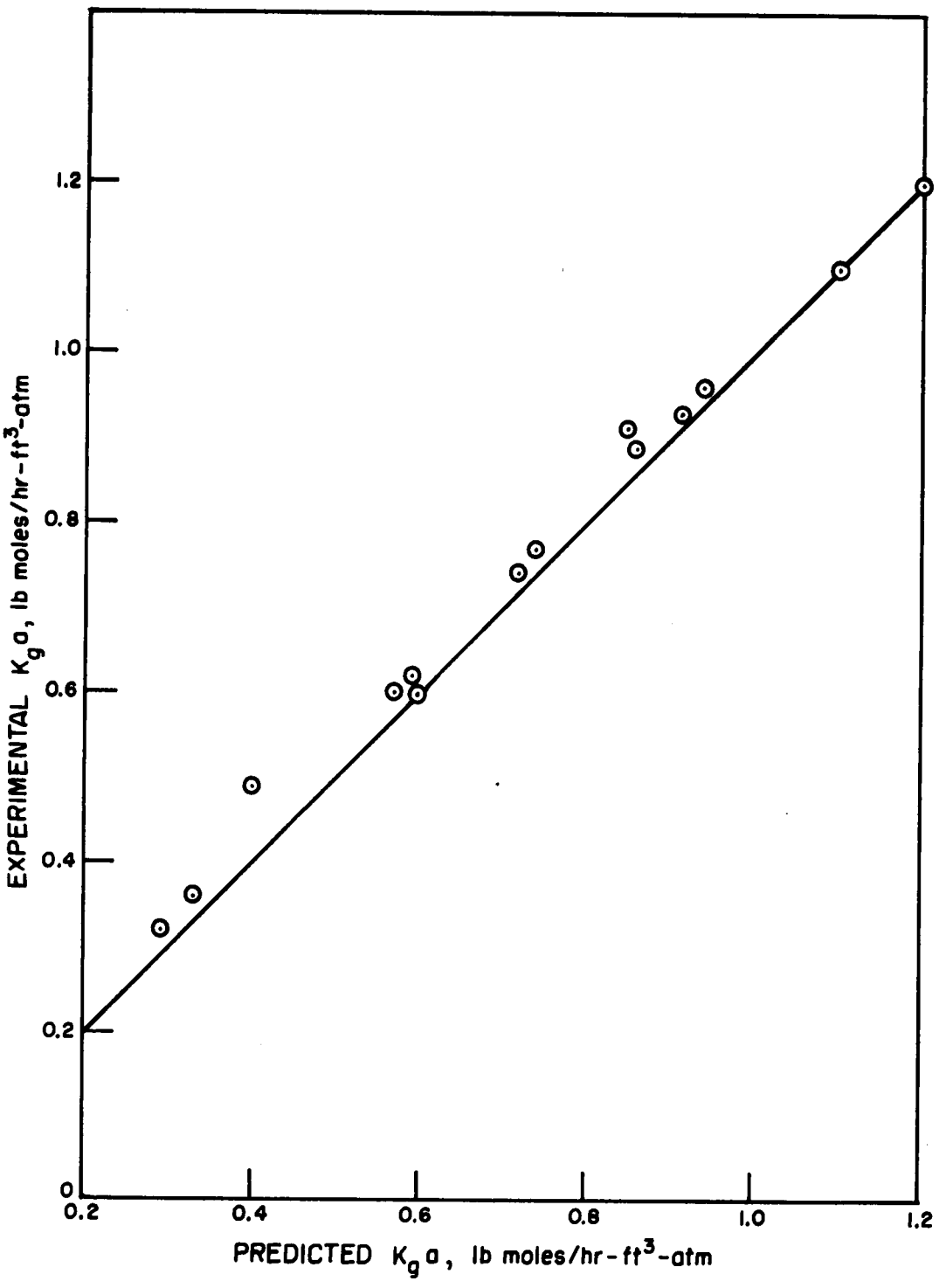


Figure 16. Comparison of Actual and Predicted Total Gas-Phase Mass-Transfer Coefficients.

behavior of the dilute component in the column. The use of the design approach is discussed more completely in the Appendix.

V. SUMMARY

The $K_g a$ and $K_g a^*$ values listed in Table XIX, page 83, can be used again to illustrate the contribution of the bulk transfer of the dilute component to its total transfer in any particular experiment. For example, in test 4, only 7 percent of the total Kr absorption was due to bulk transfer, whereas, for tests 5 and 6, the bulk transfer contributions were 13 and 31 percent, respectively. Thus, it is apparent that if bulk transfer due to carrier coabsorption is ignored, significant errors might occur in the prediction of dilute component transfer.

Finally, the whole phenomenon of carrier gas coabsorption deserves, perhaps, some additional, more general comment. An obvious question is: Why choose a solvent, or why choose absorber operating conditions, which result in carrier gas coabsorption? This is a pertinent question, since one obvious impact of such choices on the overall process is the requirement of an intermediate stripper column to deal with the coabsorbed carrier. The answer is based on the fact that in the selective absorption process for Kr and Xe, the overriding consideration is achieving virtually total removal of the noble gases. Thus, one of the most important criteria in solvent selection is the absolute solvent capacity for Kr and Xe, rather than discrimination between noble gases and carrier gases. When additional factors are considered, such as thermal and radiation stability, toxicity, flammability, and so on, one is led to conclude that CCl_2F_2 is an excellent solvent for Kr-Xe

removal processes, in spite of the added process complexities. A consequence of this, as has been illustrated, is frequently significant carrier gas coabsorption. However, as shown in this chapter, carrier coabsorption is not totally unproductive, since coabsorption also contributes--sometimes substantially--to the overall absorption of Kr and Xe.

CHAPTER VII

MIXED CARRIER GAS MASS-TRANSFER DATA

I. INTRODUCTION

In the previous chapter, the gas mixture considered was a binary consisting of a dilute component plus a coabsorbing carrier. Because of the carrier transfer, the problem represented there was an elementary multicomponent absorption problem. The problem is designated as elementary since the transfer of the two gases is controlled in different phases. That is, carrier transfer is liquid-phase controlled, and dilute component transfer is gas-phase controlled, in the context of the usual film theory concepts. The consistency of the results in the previous chapter suggests the absence, in this particular system, of significant component interactions in either phase beyond those accounted for either by the design approach itself or by the estimating techniques used for K_i^* values in mixed systems (cf. page 28).

The experiments with air represent another elementary multicomponent transfer situation in which the single dilute component transfer is from a carrier gas mixture comprised now of two coabsorbing carrier gases. Most of the work done on multicomponent systems has been with another, in some respects more complicated, class of problems, characterized by two or more very soluble dilute components transferring through an insoluble carrier. In the latter case, gas-phase interactions often have to be accounted for, and this usually requires approximations, since the rigorous convective transport equations are

often intractable when the number of components exceeds two. One successful approach for two dilute components and a third insoluble carrier appears to be that of Toor and Sebulsky (Toor and Sebulsky, 1961).

Notwithstanding the mathematical difficulties, gas-phase interactions in multicomponent transfer situations can at least be qualitatively represented from the Stefan-Maxwell equations and frequently approximated with acceptable accuracy. However, for the general problem considered here, there is not a great deal of theory available to help resolve any liquid-phase interactions if they should occur. Of course, the suggestion from the results of the previous chapter was that unusual interactions were absent in either phase for the systems being investigated. The purpose of this analysis was to determine whether this is still the case when a third gaseous component is added. It should be noted that in these CCl_2F_2 systems, relatively high loadings (up to 10 mole percent) of the solvent are achieved due to carrier absorption. At these loadings, where one molecule out of 10 is some solute molecule, confirmation of the absence of significant interactions is of practical interest in terms of helping further to identify the regions in which this design package is adequate.

II. ANALYSIS OF AIR TESTS

Experimental series 15, 16, and 17 involved use of air as the carrier gas. If there are not significant interactions, then one should be able to treat air as a pure gas with linearly additive properties based on its composition, rather than deal individually with N_2 and O_2.

In the first analysis of the test data, K_La values for N_2 and O_2 were separately estimated on the basis of the previous data for N_2 and Ar. In the second analysis, the reported mixture properties of air were used to estimate K_La's. In Table XXI, a comparison is given which shows how well both approaches match the experimental data. The numerical calculations were started at the top of the column, where the solute mole fractions in the solvent were equal to zero, so the comparison parameters shown are the predicted and actual column inlet gas flows. In all cases, agreement was within 4 percent. While both approaches proved adequate, the advantage of considering air as a pure gas in these cases is computational simplicity, while use of separate N_2 and O_2 constants will establish concentration profiles for each of the gases if such information is desired. Figure 17 illustrates the gradients calculated in this manner for run 15.

Based on these results, it is apparent that, for the systems of interest in this work, having a carrier which is a mixture of coabsorbing gases does not really complicate the mass-transfer problem, except computationally, and that carrier absorption can be adequately predicted on either an overall or component basis.

III. EXTENSION OF RESULTS

With the preceding analysis indicating that air carrier systems can be handled in a straightforward manner, a final objective was to extend the various results of this dissertation to experimental conditions as far removed as possible from those used in its development. As shown in Table XXII, Stephenson and co-workers have published

TABLE XXI

Summary of Air Test Results

Series	$K_L a$, hr^{-1}			Column Inlet Gas Flow, lb mole/hr		
	N_2	O_2	Air	Using N_2, O_2 $K_L a$ Values	Using Air $K_L a$ Value	Measured
15	32	38	33	0.917	0.915	0.922
16	32	38	33	0.788	0.791	0.768
17	30	36	31	0.817	0.828	0.799

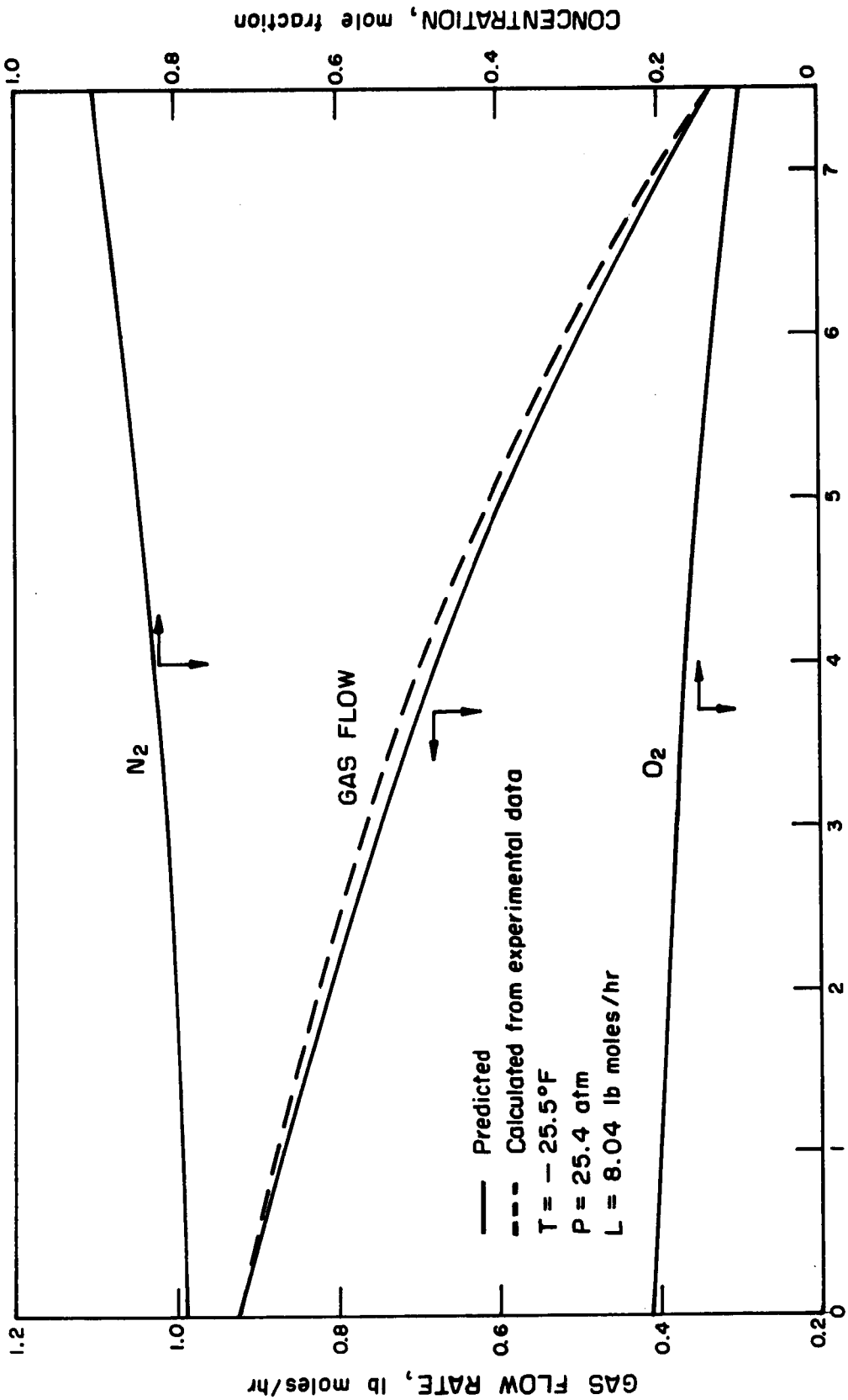


Figure 17. Concentration and Gas Flow Profiles for Test 15.

TABLE XXII

Comparison of Absorption Experiments Using CCl_2F_2 Solvents

Absorption Parameter	Parameter Range	
	This Work	Stephenson, et al.
Temperature, °F	-35 to -23.7	-76.7 to -21.2
Pressure, atm	21.4 to 28.7	11.1 to 29.7
Inlet Solvent Flow, gpm	0.98 to 1.3	0.98 to 1.63
Inlet Gas Flow, scfm	2.83 to 9.72	9.5 to 22.3
Carrier Gases Used	He, N_2, Air, Ar	Air
Dilute Gases Used	Kr, Xe	Kr

Sources: This work; Stephenson, et al., 1970.

absorption test results, using CCl_2F_2 as the solvent and air as the carrier, covering much wider ranges of temperatures, pressures, and flows than were employed in this work (Stephenson, et al., 1970). Accordingly, it was decided to apply the methods developed in this dissertation to each of Stephenson's experiments and compare the resulting predictions with the experimental results.

In checking the carrier gas behavior, equation (37), page 73, was used to estimate K_La values for N_2 and O_2. For Kr, the K_ga^* correlation, equation (44), page 85, was used together with equations (46) and (47) to estimate K_ga values. In applying equation (44), the shortcut of assuming an average gas flow rate equal to 80 percent of the inlet rate was taken. Again, for the carrier gas, the computational procedure provided estimates of the column inlet gas flow rates, starting from the exit conditions. For Kr, the comparison parameter was the Kr removal percentage.

The results of the comparison are listed in Table XXIII, along with other run data and the predicted mass-transfer coefficients. For the carrier gas, the gas inlet flows were predicted very closely, with an average difference between the two sets of numbers of about 7 percent. The Kr absorption data also agreed very well, although a few of the numbers for the runs with low removal efficiencies were off some. This can be explained by the fact that in some of Stephenson's tests, Kr was not completely removed from the CCl_2F_2 in the stripper column, and this, in turn, limited the Kr removal efficiency in the absorber. In making this comparison, however, it was assumed that no Kr was present in the lean solvent. As a final point, the error introduced by using the

TABLE XXIII

Extension of Results to Stephenson's Experiments

Run	T, °F	P, atm	Predicted $K_L a$, hr^{-1}		Predicted Kr $K_g a$, lb moles/hr-ft^3-atm	Flows, lb moles/hr				Kr Absorption, %	
						Solvent In	Gas Out	Gas In			
			N_2	O_2				Measured	Predicted	Measured	Predicted
1	-24.0	28.3	25.4	26.8	0.859	6.01	0.856	1.40	1.36	99.7	99.3
2	-25.0	28.3	25.2	26.7	0.875	6.02	0.917	1.42	1.44	99.8	99.1
3	-30.2	28.3	24.5	25.9	1.49	6.04	1.60	2.26	2.10	97.5	97.3
4	-32.5	28.3	24.2	25.6	1.44	6.08	1.44	2.23	1.96	98.5	98.6
5	-30.7	28.3	24.4	25.8	2.06	6.05	2.40	3.06	2.90	75.0	88.9
6	-26.3	28.3	30.3	32.1	1.50	8.04	1.49	2.25	2.14	98.7	99.1
7	-26.3	28.3	30.4	32.2	1.53	8.05	1.51	2.29	2.16	99.2	99.1
8	-24.0	29.7	30.8	32.6	1.35	8.03	0.997	2.21	1.68	99.7	99.9
9	-23.0	29.5	30.9	32.7	1.40	8.02	1.05	2.26	1.72	99.8	99.9
10	-23.0	23.0	30.9	32.7	1.78	8.02	1.44	2.18	1.96	96.4	98.3
11	-22.0	23.0	31.1	32.9	1.79	8.01	1.45	2.19	1.96	96.6	98.2
12	-25.5	23.0	35.4	37.5	1.82	10.1	1.38	2.21	2.00	98.5	99.4
13	-26.0	17.7	30.4	32.2	2.45	8.04	1.59	2.10	1.99	88.3	94.2
14	-26.0	17.7	30.4	32.2	2.27	8.04	1.68	2.17	2.08	84.2	90.3
15	-26.0	17.7	30.4	32.2	2.36	8.04	1.57	2.14	1.96	89.9	94.5
16	-43.2	17.7	27.5	29.2	2.63	8.18	1.88	2.32	2.28	87.2	94.7
17	-44.7	17.7	27.3	28.9	2.60	8.20	1.88	2.31	2.27	85.6	95.0
18	-41.3	17.7	27.8	29.5	2.72	8.16	1.92	2.34	2.31	85.0	93.9
19	-52.7	17.7	30.1	31.9	2.51	10.3	1.71	2.28	2.17	98.8	98.9
20	-50.0	17.9	21.8	23.1	2.42	6.19	1.92	2.33	2.24	73.6	87.8

TABLE XXIII (continued)

Run	T, °F	P, atm	Predicted $K_L a$, hr^{-1}		Predicted Kr $K_g a$, lb moles/hr-ft^3-atm	Flows, lb moles/hr				Kr Absorption, %	
						Solvent In	Gas Out	Gas In			
			N_2	O_2				Measured	Predicted	Measured	Predicted
21	-53.5	17.7	21.3	22.6	2.50	6.20	2.02	2.38	2.34	73.2	86.9
22	-52.2	11.1	26.1	27.6	4.00	8.26	1.95	2.27	2.20	71.5	79.3
23	-22.8	22.2	31.0	32.8	2.01	8.02	1.66	2.31	2.16	90.6	96.6
24	-21.2	22.2	31.3	33.1	1.88	8.02	1.51	2.21	2.02	96.2	97.5
25	-26.3	21.4	25.1	26.6	1.78	6.04	1.65	2.13	2.04	86.0	89.0
26	-27.0	21.4	24.9	26.4	1.81	6.03	1.72	2.17	2.13	80.8	87.6
27	-29.3	28.3	24.6	26.1	1.42	6.05	1.45	2.20	1.96	96.8	98.2
28	-75.5	24.6	22.4	23.7	1.70	8.46	1.15	2.12	1.68	99.6	99.9
29	-76.7	11.1	22.2	23.5	4.23	8.46	2.02	2.38	2.26	84.9	86.3
30	-74.3	21.4	22.6	23.9	2.02	8.45	1.66	2.27	2.12	99.2	99.5
31	-73.3	18.1	22.7	24.1	1.50	8.44	0.905	1.53	1.30	99.9	99.9
32	-71.5	18.1	23.0	24.4	1.49	8.43	0.894	1.53	1.29	99.9	99.9
33	-71.7	18.1	18.9	20.0	3.68	6.30	2.93	3.29	3.25	73.7	81.8
34	-75.3	18.1	18.5	19.6	3.75	6.34	2.99	3.35	3.31	75.6	83.2

Source: Stephenson, et al., 1970.

shortcut mentioned above to estimate the average gas flow rate was spot-checked by redoing some of the comparisons using the true averages. This resulted in predicted Kr removal percentages of 98.2 versus 98.3 with the shortcut for run 10, 94.8 versus 94.5 for run 15, 89.1 versus 87.8 for run 20, 90.0 versus 89.0 for run 25, and so on. In any event, the overall results of the comparison are very favorable, especially when one realizes that all elements of the design package, including the predictive equations for physical properties, diffusion coefficients, and equilibrium coefficients, as well as the mass-transfer correlations, were being tested.

As a final check, some abbreviated air carrier tests were conducted with attempts made to withdraw gas samples between each section of the column, as well as at the ends. These were not complete experiments, but focused only on the Kr concentration profiles. While the accuracy of this data is somewhat uncertain, it is presented in Figure 18, along with the Kr profiles predicted using the techniques developed in this dissertation. Again, the agreement was good, with the terminal points and all but one of the intercolumn points matched closely.

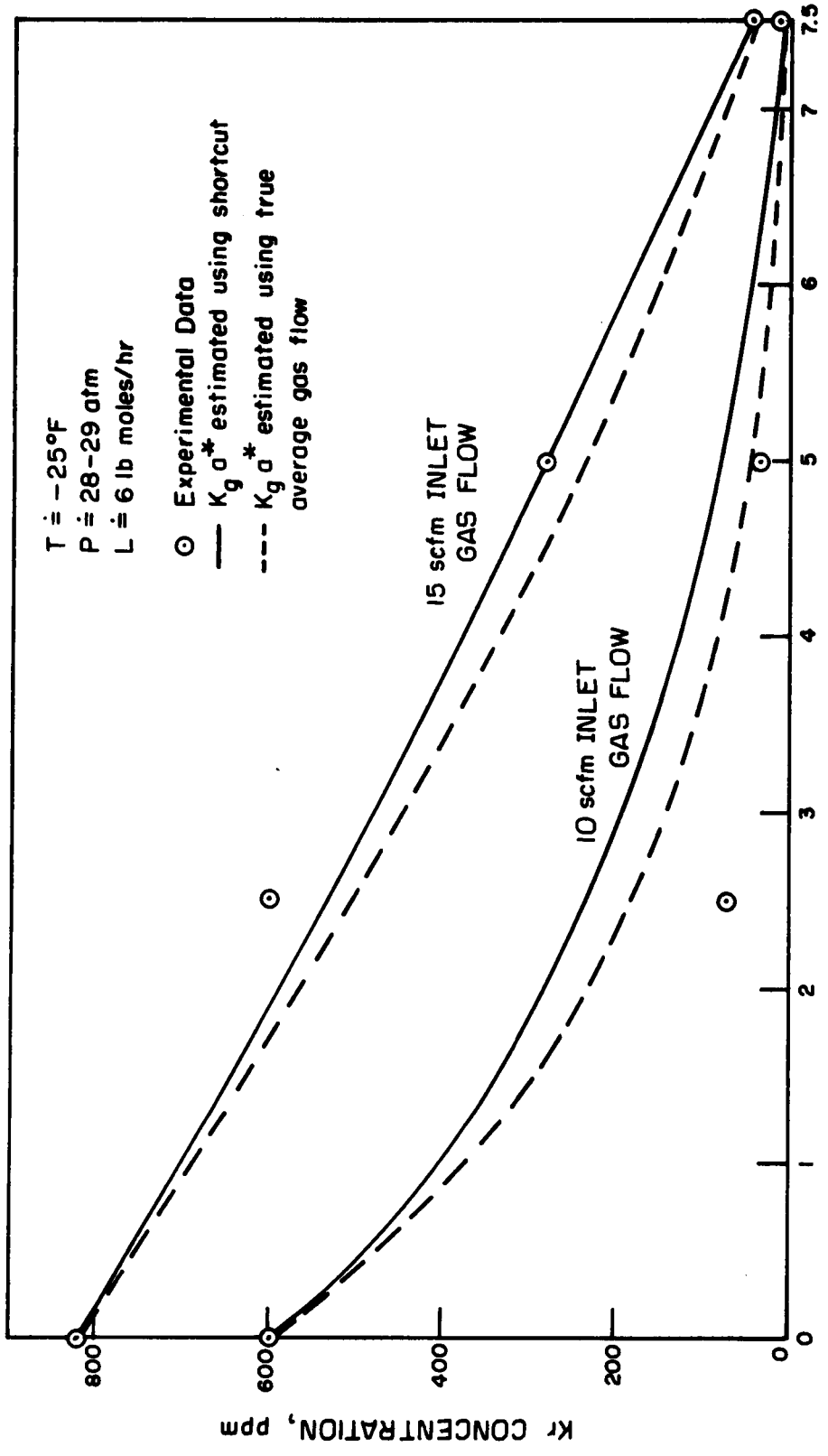


Figure 18. Kr Concentration Profiles.

CHAPTER VIII

CONCLUSION

It was noted earlier that the fluorocarbon absorption process appears useful for Kr-Xe removal at nuclear facilities and also has the potential for application to a number of other gas scrubbing problems. The fact that fluorocarbon systems, particularly when CCl_2F_2 is used as the solvent, are considerably different in many properties than more common absorption systems prompted the development of a design package, based on the film theory framework, which addressed the specific problem of multicomponent gas absorption in systems having carrier gases which coabsorb with the desired solutes.

Table XXIV compares the key parameters typical of fluorocarbon absorption problems with those of a more common system, air-CO_2-water. While many of the differences are substantial, the one which is most significant is the unusually high solubility of the carrier gas in the CCl_2F_2 system. Because of this, dilute component transfer is from a coabsorbing, rather than insoluble, carrier.

The primary results of this dissertation are as follows:

1. Methods have been selected for estimating the various fundamental fluid properties for CCl_2F_2-gas mixture systems. Since the CCl_2F_2 absorption process is normally operated at temperatures and pressures which are somewhat removed from the regions where most physical property data are best known, this effort was considered necessary. The methods chosen appeared to give acceptable results.

TABLE XXIV

Comparison of Kr-Air-CCl_2F_2 and CO_2-Air-Water Systems

Parameter		Kr-Air-CCl_2F_2	CO_2-Air-Water
Typical Temperature, °F		-25	77
Typical Pressure, atm		25	1
Packing Type Studied		mesh	rings
Equilibrium Constants, atm:	Carrier	250	70,000
	Dilute	70	1,000
Schmidt Numbers (Liquid-Phase)		35	670

2. It was found that the small amount of reported solubility data for N_2, O_2, and Ar in CCl_2F_2 was not adequate to support this dissertation. As a result, techniques, based on Hildebrand's regular solution theory, were selected for estimating the necessary equilibrium constants. The estimates appeared to be acceptably consistent and certainly proved to be satisfactory for use in the mass-transfer developments of this dissertation. It was concluded that the regular solution theory framework provides a useful way to estimate equilibrium constants for the particular systems investigated in this study.
3. Experiments with essentially pure carrier gases were conducted to obtain data on carrier transfer. These data were correlated and the correlations were used to account for carrier gas coabsorption, with acceptable results.
4. A picture was presented which describes the mass-transfer of dilute components as a conventional diffusive transfer superimposed on a net flux caused by carrier transfer. Supporting equations were developed which quantitatively related the total mass-transfer coefficient of a dilute component to both its diffusive transfer coefficient and the carrier gas mass-transfer coefficient. The diffusive mass-transfer coefficients for the dilute components were correlated, and the basic relationship proposed between the various coefficients was successfully tested. As a result, it was shown that, for a given dilute gas-carrier gas system,

dilute gas mass-transfer could be directly related to carrier gas coabsorption.

5. The results of this study indicated that significant gas-phase and liquid-phase component interactions are absent in this particular system up to the limits investigated.
6. It was shown that the complete design package for CCl_2F_2 absorption systems could be extended to conditions well removed from those of its development, with good results.
7. Finally, it was generally established that the film theory framework could be used, with appropriate modifications, to develop a valid absorber design approach for multicomponent systems characterized by carrier gas coabsorption.

LIST OF REFERENCES

LIST OF REFERENCES

Adler, S. B., et al., "Thermodynamic Consistency of Binary Liquid-Vapor Equilibrium Data When One Component is Above Its Critical Temperature," AIChE J., 6, 104 (1960).

Bird, R. B., et al., Transport Phenomena, John Wiley and Sons, Inc., New York (1960).

Bragg, E. J., "How to Design a Goodloe Column," Packed Column Company, Metex Corporation, Technical Bulletin, Edison, New Jersey (1972).

Bretsznajder, S., Prediction of Transport and Other Physical Properties of Fluids, Pergamon Press, Oxford, England (1971).

E. I. du Pont de Nemours and Company, Inc., "Thermodynamic Properties of Freon-12 Refrigerant," Technical Bulletin T-12, Wilmington, Delaware (1956).

Hildebrand, J. H., "Thermodynamic Parameters for Dissolved Gases," Proc. Nat. Acadam. Sci. U. S., 64, 1331 (1969).

Hildebrand, J. H., and H. Hirakoa, "Solubility and Entropy of Solution of Certain Gases in $(C_4F_9)_3N$, $CCl_2F.CClF_2$, and 2, 2, 4-$(CH_3)_3C_5H_9$," J. Phys. Chem., 68, 213 (1964).

Hildebrand, J. H., and R. H. Lamoreaux, "Solubility of Gases in Liquids: Fact and Theory," Ind. Eng. Chem. Fundamentals, 13, 110 (1974).

International Critical Tables, III, 1st Edit., 204, McGraw-Hill, New York (1928).

Linford, R. G., and J. H. Hildebrand, "Solubility and Entropy of Solution of Gases in $CCl_2F.CClF_2$," Trans. Faraday Soc., 66, 577 (1970).

McHarness, R. C., et al., "The New Thermodynamic Properties of Freon-12," Refrigerating Engineering, 63, 9, p. 31 (1955).

Merriman, J. R., "Estimation of Irradiated Reactor Fuel Properties for Reprocessing Studies," M.S. thesis, The University of Tennessee, Knoxville (1966).

Merriman, J. R., et al., "Removal of ^{85}Kr from Reprocessing Plant Off-Gas by Selective Absorption," USAEC Report K-L-6201, Oak Ridge, Tennessee (1972).

Merriman, J. R., et al., "Process for the Separation of Components from Gas Mixtures," U. S. Patent 3,762,133 (1973).

Merriman, J. R., et al., "Recovery of Purified Helium or Hydrogen from Gas Mixtures," U. S. Patent 3,785,120 (1974).

Merriman, J. R., and J. H. Pashley, "Engineering Development of an Absorption Process for the Concentration and Collection of Kr and Xe," USAEC Report K-1745, Oak Ridge, Tennessee (1968).

Perry, R. H., and C. H. Chilton, (Eds.), Chemical Engineer's Handbook, 5th Edit., McGraw-Hill, New York (1973).

Powell, R. J., "Solubility of 16 Gases in $(C_4F_9)_3N$ and CS_2," J. Chem. Eng. Data, 17, 302 (1972).

Prausnitz, J. M., Molecular Thermodynamics of Fluid-Phase Equilibria, Prentice-Hall, Inc., Englewood Cliffs, New Jersey (1969).

Prausnitz, J. M., and F. H. Shair, "A Thermodynamic Correlation of Gas Solubilities," AIChE J., 7, 682 (1961).

Steinberg, M., "The Recovery of Fission Product Xe and Kr by Absorption Processes," USAEC Report BNL-542, Brookhaven National Laboratory, Long Island, New York (1959).

Stephenson, M. J., et al., "Experimental Investigation of the Removal of Kr and Xe from Contaminated Gas Streams by Selective Absorption in Fluorocarbon Solvents: Phase I Completion Report," USAEC Report K-1780, Oak Ridge, Tennessee (1970).

Toor, H. L., and R. T. Sebulsky, "Multicomponent Mass-Transfer," AIChE J., 7, 558 (1961).

Wilke, C. R., and P. Chang, "Correlation of Diffusion Coefficients in Dilute Solutions," AIChE J., 1, 264 (1955).

Yamamoto, Y., and H. Takeda, "Solubility of ^{85}Kr in Some Organic Solvents," J. Fac. Eng. U. Tokyo, A-7, 44 (1970).

Yen, L. C., and J. J. McKetta, Jr., "A Thermodynamic Correlation of Nonpolar Gas Solubilities in Polar, Nonassociated Liquids," AIChE J., 8, 501 (1962).

APPENDIX

APPENDIX

SUMMARY OF CALCULATIONAL PROCEDURES

I. EXPERIMENTAL DATA REDUCTION

Consider a typical absorption test. Prior to reduction of the experimental data, the necessary physical properties and equilibrium constants were estimated using the methods presented in Chapter II. With the terminal mole fractions, x_1, known from the run data, the next step was to obtain the mass-transfer coefficient for the carrier gas using equation (35), repeated below:

$$\frac{K_L a \rho_M S Z}{L_2} = \frac{1}{1 - x^*}\left[\frac{1}{1 - x^*}\ln\left(\frac{x^*(1 - x_1)}{x^* - x_1}\right) - \frac{x_1}{1 - x_1}\right] . \qquad (35)$$

For purposes of condensation of this presentation, the units for the factors in equation (35) and subsequent equations will not be repeated in this Appendix, since the factors appear elsewhere, are conventional, and, by now, are also familiar. To provide assistance, however, the original equation numbers will be continued here. As noted previously, equation (35) applies to situations where the carrier gas is a single pure gas and where the mole fractions of the contained dilute species are extremely low (10^{-6} to 10^{-9} in this work).

With $K_L a$ known, equation (35) was reapplied using values of z ranging from z = 0 to z = Z, instead of Z, in the left-hand side. The increment was $\Delta z/2$, where Δz in these particular calculations was Z/10.

For each value of the left-hand side, a corresponding x (instead of x_1) was obtained by trial and error. The Newton-Raphson method was used here, requiring the derivative of the right-hand side of equation (35), which is:

$$f'(x) = \frac{1}{(1 - x)^2(x^* - x)} \quad . \tag{48}$$

This provided values of x(z) for the carrier gas from the top to the bottom of the column at every $\Delta z/2$ increment.

Using the x(z) values, the carrier gas material balance equation was next solved to obtain corresponding G(z) numbers, viz:

$$G(z) = G_2 + \frac{x(z)L_2}{1 - x(z)} \quad , \tag{49}$$

in terms of liquid and gas flows at the top of the column (identified as point 2). Equation (49) is based on the assumption that the lean solvent feed contains no dissolved carrier gas, which was valid for the experiments presented in this dissertation.

Next, the diffusive mass-transfer coefficient for the dilute gas was obtained. The starting equation was equation (42), also represented below:

$$d(Gy) - ydG = K_g a^* SP(y - y^*)dz \quad , \tag{42}$$

which gives

$$Gdy = K_g a^* SP(y - mx)dz \quad , \tag{50}$$

where the mole fractions here are for the dilute gas. Incorporating the dilute component material balance relationship in equation (50) gives:

$$dy = \frac{K_g a^* SP}{G} \left[y - m\left(\frac{Gy - G_2 y_2}{G + L_2 - G_2} \right) \right] , \qquad (51)$$

again in terms of flows at the top of the column. Now, at the top of the column, $x = 0$. Also, for each run, the inlet concentration of dilute gas, y_1, and the ratio of the inlet and outlet concentrations, y_1/y_2, were known. A starting value of $K_g a^*$ was assumed. Then, a fourth-order Runge-Kutta scheme was used to predict a value of y_1, starting from the column top and computing y's at each Δz increment. This required the previous G(z) data (in increments of $\Delta z/2$). The calculations were straightforward, as long as one remembered to use the appropriate values of G(z) in computing each of the Runge-Kutta constants. Once a predicted y_1 was obtained, the resulting y_1/y_2 ratio was compared with the experimental value. If these numbers did not agree satisfactorily (within 0.1 percent in this work), the $K_g a^*$ was adjusted on the basis of the difference and the procedure repeated until a value of $K_g a^*$ was obtained which gave satisfactory agreement. No record was maintained on the number of iterations required.

The final step in the data reduction process was calculation of the total mass-transfer coefficient for the dilute component. The starting point was the gas design equation, equation (29), which is repeated here:

$$d(Gy) = K_g aSP(y - y^*)dz . \qquad (29)$$

As before, the dilute component material balance was incorporated:

$$d(Gy) = K_g aSP \left[y - m\left(\frac{Gy - G_2 y_2}{G + L_2 - G_2} \right) \right] , \qquad (52)$$

and, additionally, the formal transformation was made:

$$d(Gy) = K_g aSP \left[\frac{Gy}{G} - m\left(\frac{Gy - G_2 y_2}{G + L_2 - G_2} \right) \right] . \qquad (53)$$

Equation (53) was also solved using a fourth-order Runge-Kutta scheme, starting with an assumed value of $K_g a$. In this case, the predicted variable was $G_1 y_1$, at the bottom of the column, so division of this quantity by the known G_1 was required before the comparison of the predicted and experimental values of y_1/y_2 could be made. Convergence criteria and procedures were the same as for the $K_g a^*$ calculations.

II. DESIGN APPROACH

The methods used to test the results of this dissertation against Stephenson's results illustrate the use of the design package in a typical absorption problem. First, for the specified conditions, the various physical properties and equilibrium constants were again estimated using the procedures given in Chapter II. Then, equation (37) was used to estimate the $K_L a$ for the carrier gas:

$$K_L a = 560\ D_L\ Re^{2/3}\ Sc^{1/2} . \qquad (37)$$

Actually, this was done for both N_2 and O_2, since the carrier in Stephenson's work was air, but to simplify this illustration it will be assumed here that there is only one carrier gas. It was shown in the

dissertation, anyway, that air could be treated as a single pure carrier, if desired, with acceptable results.

Next, the total mass-transfer coefficient for the dilute component was estimated using:

$$K_g a^* = \frac{0.71 \langle G \rangle^{1.22}}{p^{1.09}} , \tag{44}$$

$$\left(\frac{y_A \Delta X_B}{\Delta y_A}\right)_{avg} = \frac{1}{2m_B}\left[1 + \frac{L_2 + G_D - m_B G_D}{L_2 + G_D - m_A G_1}\right] , \tag{47}^4$$

and, finally,

$$(K_g aP)_A = (K_g a^* P)_A + (K_L a \rho_M)_B \left(\frac{y_A \Delta X_B}{\Delta y_A}\right)_{avg} . \tag{46}^4$$

Then, the carrier gas coefficient, $K_L a$, was converted to an equivalent gas-phase-based coefficient, $(K_g a)_B$, using:

$$(K_g a)_B = \frac{\rho_M K_L a}{K_B^*} . \tag{34}$$

At this point, difference versions of the gas-phase design equation, equation (29), were set up for both the carrier and the dilute component:

$$\Delta(Gy)_j = (K_g a)_j SP\ (y - y^*)_j\ \Delta z , \tag{54}$$

---

[4] It should be remembered that equations (46) and (47) apply to a binary gas mixture comprised of a carrier gas plus a dilute gas. For other cases, similar equations can be obtained, although the author found it more convenient to limit this exercise to obtaining analogs of equation (46) and just used the experimental concentrations directly instead of developing n-component analogs of equation (47).

where j takes on values of A and B corresponding to dilute gas and carrier gas, respectively, and where the y_j^* are obtained using the equilibrium constants and component material balances.

The calculations were started from the top of the column, where the $x_j = 0$, and used to predict $(Gy)_j$ values at each Δz increment down the column. These results were used to give G(z) values, since $\Sigma(Gy)_j = G$, and also, with the material balances, to give $x_j(z)$ values. The increment size, Δz, was chosen to be much smaller here than for the previous Runge-Kutta calculations, since this technique is not as sophisticated. Accordingly, a $\Delta z = Z/100$ was used.

In some spot checks, the mass-transfer coefficients were separately calculated using the appropriate correlations at each point Δz apart in the column together with the corresponding flows rather than using average values. This appeared to make virtually no difference for the carrier gas and very little difference for the dilute gas.

Finally, of course, in a typical design problem knowledge of all the conditions is not as clear as just described. Usually, one has a feed gas of known composition and is required to select an absorber which will remove a specified amount of one component and to predict what happens to the other components. In this case, the design approach becomes an iterative process, started by assuming such parameters as temperature, pressure, and L/G ratio; then going through the above calculations to establish the required column height; then repeating the cycle; and so on. Nevertheless, it is hoped that the presentation in this Appendix, together with the thoughts and results contained in the body of the dissertation, will be a useful design guide for

multicomponent absorption systems characterized by carrier gas coabsorption.

VITA

James Robert Merriman was born in Knoxville, Tennessee on November 22, 1941. He attended elementary and secondary schools in Morristown and Maryville, Tennessee, graduating from Maryville High School in 1959. He then attended Vanderbilt University and received the B.E. degree in June 1963. In September 1963, he entered the Graduate School of The University of Tennessee, receiving an M.S. degree in 1966 and a Ph.D. degree in 1975.

He is married to the former Sandra Jane Hughes, of Alcoa, Tennessee, who is also a graduate of The University of Tennessee.

His parents, Robert Lee and Evelyn Bridges Merriman, are residents of Maryville, Tennessee. He has one brother, Daniel Lee Merriman.

Since 1963, he has been employed by Union Carbide Corporation, Nuclear Division, Oak Ridge, Tennessee. He is currently manager of engineering at the Paducah Gaseous Diffusion Plant.

He is a member of the American Institute of Chemical Engineers.